Engineering Geology 294 (2021) 106398

Contents lists available at ScienceDirect

Engineering Geology

journal homepage: www.elsevier.com/locate/enggeo

Inferring precipitation thresholds of landslide activity from long-term dendrochronological and precipitation data: Case study on the unstable slope at Karpenciny, Poland

Małgorzata Wistuba [a,*], Elżbieta Gorczyca [b], Ireneusz Malik [a]

[a] University of Silesia in Katowice, Faculty of Natural Sciences, Institute of Earth Sciences, Polish-Chinese Centre for Environmental Research, ul. Będzińska 60, 41-200 Sosnowiec, Poland
[b] Jagiellonian University in Kraków, Institute of Geography and Spatial Management, ul. Gronostajowa 7, 30-387 Cracow, Poland

ARTICLE INFO

Keywords:
Precipitation threshold
Landslide reactivations
Landslide causes
Tree-ring reconstruction

ABSTRACT

An extended statistical comparison of numerous precipitation parameters (absolute, minimum, and maximum totals; number of days with precipitation; and duration of precipitation in particular months, seasons, and longer periods) and the 48-y long dendrochronological reconstruction of landslide activity was conducted for a generally unmonitored landslide slope at Karpenciny, Western Carpathians, Poland. The Karpenciny landslide is a deep (approximately 40 m) translational landslide consisting of large, poorly fragmented, and almost intact landslide blocks. It is located only 2.4 km from the meteorological gauging station. We aimed to explore the long-term dependence of this landslide on precipitation conditions and reveal the precipitation parameters crucial for its activity, that is, direct triggers and preparatory antecedent precipitation. Therefore, dendrochronological records of tree-ring eccentricity and compression wood in 35 Norway spruce trees were correlated with 520 precipitation parameters (including seasonality, duration, and total), which might influence the activity of the studied landslide. Ten best-correlated precipitation parameters and seasonal sums of summer half-years and preceding winter half-years (separately and in total, i.e. as 12-month sums), were then tested for their potential in establishing precipitation thresholds for landslide activity. The analysis of multiple precipitation parameters enabled us to develop precipitation thresholds based on both direct causes and long-term preparatory precipitation necessary to accelerate the studied landslide. From the tree-ring data, we established landslide-safe conditions and 0.5-probability thresholds for a particular landslide slope. This study also generated comprehensive data on the seasonality of antecedent and triggering precipitation, long-term periods of antecedent precipitation, critical minimum levels of precipitation that sustain slope imbalance, and the importance of generally wet conditions (demonstrated as a high total number of days with precipitation regardless of its totals) as a factor in landslide activity. These patterns of landslide-precipitation dependence would not have been revealed with standard methods and standard precipitation parameters applied in threshold analyses. Thus, long-term reconstructions can be a valuable source of data for precipitation thresholds of landslide activity.

1. Introduction

Precipitation thresholds are commonly applied as indicators of precipitation levels which pose a threat to landslide reactivations (Guzzetti et al., 2007; Segoni et al., 2018). The concept has already been explored for over five decades (Endo, 1969; Campbell, 1975), with abundant examples of thresholds established in various mountainous areas and for landslides of diverse relief, structure, and geological settings (Crosta and Frattini, 2001; Brunetti et al., 2010; Bíl et al., 2016; Garcia-Urquia, 2016; Remaître and Malet, 2017; Saito et al., 2017; He et al., 2020; Yang et al., 2020). However, for most of these established precipitation thresholds, the data on landslide activity usually cover 5–20 years (Segoni et al., 2018). Longer, more representative and reliable datasets are rarely involved (Giannecchini, 2005; Lagomarsino et al., 2013; Rosi et al., 2015; Garcia-Urquia, 2016). Datasets with observations from more than one landslide slope can be extended (Brunetti et al., 2010; Martelloni et al., 2012; Peruccacci et al., 2012, 2017; Segoni et al., 2014a; Bíl et al., 2016; He et al., 2020). However, this can result in

* Corresponding author.
E-mail address: malgorzata.wistuba@us.edu.pl (M. Wistuba).

https://doi.org/10.1016/j.enggeo.2021.106398
Received 24 March 2021; Received in revised form 16 September 2021; Accepted 20 September 2021
Available online 25 September 2021

serious generalisation. Moreover, precipitation thresholds are mainly based on landslide inventories which only include the most severe events of slope activity (Giannecchini, 2005; Brunetti et al., 2010; Garcia-Urquia, 2016; He et al., 2020; Yang et al., 2020) available for direct, naked-eye observations. Diagnosing the causes of such strong events is crucial because of the consequent losses and damages. However, such inventories are fragmentary compared to the entire range of landslide activity, which includes not only sudden and strong displacements but also smaller accelerations and periods of stability (e.g., Xu et al., 2020).

The above-mentioned issues result mainly from limited access to systematic and continuous monitoring of landslide activity. Regular observations and measurements of landslide movement covering periods of more than two decades remain rare (Giannecchini, 2005; Behling et al., 2016; Gullà et al., 2018). Thus, long-term datasets often combine information from various sources and monitoring methods (Palis et al., 2017; Gullà et al., 2018; Carlà et al., 2019; Wasowski and Pisano, 2020; Xu et al., 2020), thus, they are rarely utilised for precipitation thresholds (Segoni et al., 2018).

Data on landslides can also be obtained from the reconstruction of past slope activity. However, methods applied for older landslide activity, such as isotope dating, achieve only the approximate age of the most severe events (e.g., Szczygieł et al., 2019), which is not precise enough to establish precipitation thresholds. In reconstructions of recent landslide activity from archival aerial or satellite imagery (Fiorucci et al., 2011), older images are often available at irregular monthly or annual intervals (e.g., Saito et al., 2017). Moreover, temporal estimations are only possible for strong landslide events that can cause significant topography changes (Weidner et al., 2019). Modern InSAR techniques are more precise and sensitive, but they rarely generate data for more than the past 10–20 years (Colesanti and Wasowski, 2006; Wasowski and Pisano, 2020; Eker and Aydin, 2021). Thus, the above-mentioned reconstructions of landslide activity, even though applied in studies on meteorological causes of landslides (e.g., Fiorucci et al., 2011; Saito et al., 2017), are rarely involved in determining precipitation thresholds (e.g., Xu et al., 2020) owing to the poor precision of dating and limited length of datasets.

Past landslide activity can also be reconstructed using dendrochronology which provides annual precision of dating and datasets ranging from several decades to centuries (Corominas and Moya, 1999; Malik and Wistuba, 2012; Lopez Saez et al., 2013a, 2013b; Migoń et al., 2014; Malik et al., 2016). Tree-ring dating of landslide activity is commonly based on the fact that the stems of trees growing on active landslides are tilted by ground movement (Shroder Jr., 1978; Braam et al., 1987) (Fig. 1). In coniferous trees, tilting accelerates radial growth and cell differentiation on the lower side of the stems. Tilting from the upright orientation by even 1–2° (Wiedenhoeft, 2013) is sufficient for immediate development (Timell, 1986) of detectable and datable disturbances of wood anatomy, such as eccentric tree rings (Braam et al., 1987) and compression wood (Ruelle, 2014) (Fig. 1). Both features are considered particularly sensitive indicators of landslide activity, recording even minor, low-velocity displacements (Braam et al., 1987; Šilhán et al., 2012; Malik et al., 2016). They can also provide valuable information on causes of landslides (Corominas and Moya, 1999; Carrara and O'Neill, 2003; Šilhán et al., 2012; Wistuba, 2014; Wistuba et al., 2015, 2018, 2021; Owczarek et al., 2020) and have the potential for practical applications in landslide hazard analyses (Lopez Saez et al., 2013b; Łuszczyńska et al., 2019; Wistuba et al., 2019).

Moreover, dendrochronology can be a valuable source of data for precipitation thresholds of landslide activity. Using tree rings as a proxy can help to overcome the limitations of thresholds established from datasets covering short periods, combining data from more than one landslide slope, and including only the most severe events of landslide activity. The complex relationships between precipitation and

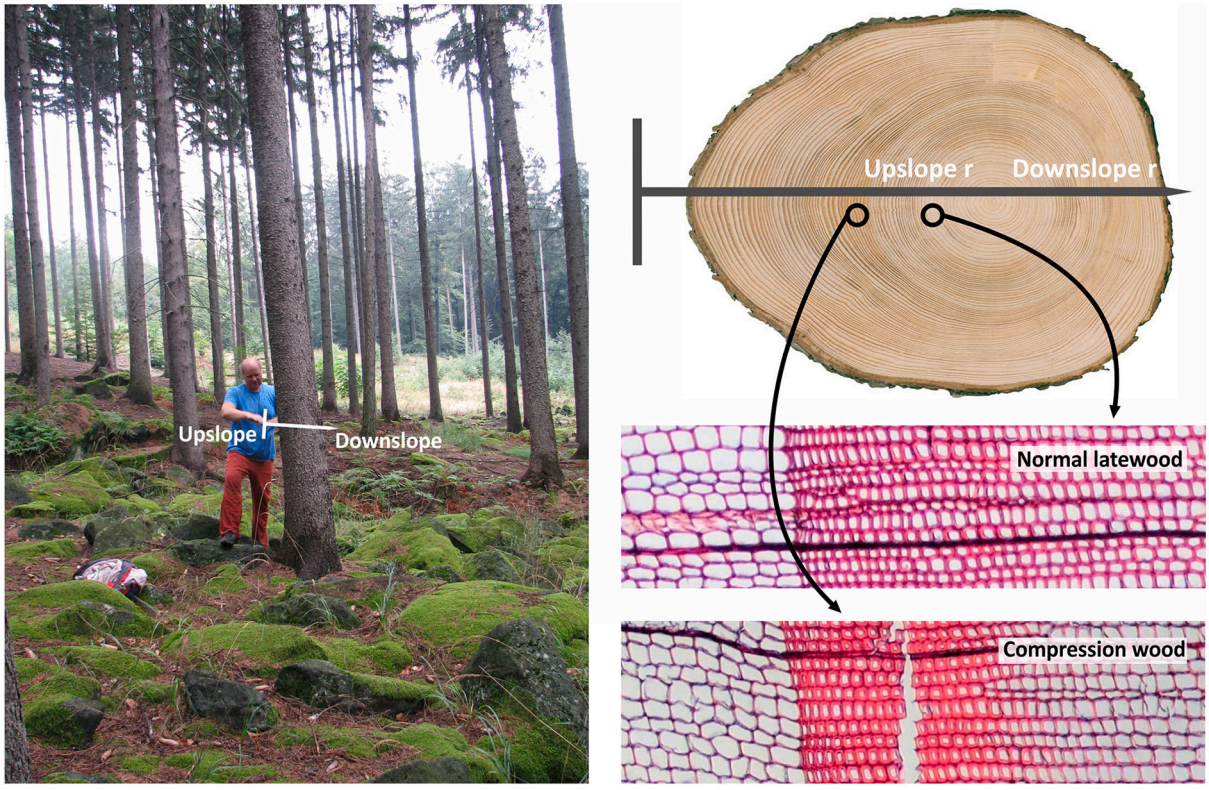

Fig. 1. Norway spruces tilted upslope on an active landslide; a stem cross-section with upslope tree-ring eccentricity (wider rings and longer total radius (r) on the upslope side of a stem) and compression wood (dark coloured rings); detailed comparison of wood anatomy of Norway spruce (*Picea abies*): normal latewood and compression wood (thicker and more rounded cell walls with smaller cell lumens).

landslides, explored through thresholds, can best be understood from long-term analyses of meteorological conditions related to all possible levels of landslide activity that change over decades between stability and abrupt accelerations. Thus, precipitation thresholds can be more reliable and better applied in hazard studies by using homogeneous, continuous, and long-term datasets on landslide activity that are obtained via dendrochronology for individual landslide slopes.

Dendrochronology has already been applied to establish meteorological thresholds for geomorphological processes, such as soil erosion (e.g., Malik et al., 2021) and debris flows (e.g. Pelfini and Santilli, 2008). However, despite the potential of dendrochronology and numerous dendrochronological studies on landslides, to the best of our knowledge, very few studies have attempted to establish precipitation thresholds for landslide activity from tree rings. For example, Lopez Saez et al. (2013b) modelled the probability of landslide reactivation in relation to seasonal precipitation totals, while Corominas and Moya (1999) and Keck et al. (2014) made preliminary attempts to establish thresholds for landslides from tree-ring data. Thus, in this study, we aimed to explore the long-term relationships between continuous changes in landslide activity and their potential meteorological causes, as demonstrated by multiple precipitation parameters. Based on a dendrochronological reconstruction covering almost 50 years, we aimed to determine the precipitation types crucial for a selected, otherwise unmonitored, landslide in the Western Carpathians, Poland. Furthermore, we aimed to test the potential of the dendrochronological analysis results to establish precipitation thresholds for landslide activity.

Although the annual resolution of dendrochronology is higher than those in other reconstruction methods, it yields only the calendar year of a landslide event (Corominas and Moya, 1999), with few examples of higher seasonal accuracy of dating (e.g., Malik and Owczarek, 2009; Lopez Saez et al., 2012). The lack of precise dating of landslide events hinders in precisely identifying the triggering factors necessary to establish precipitation thresholds. Thus, utilising the results of the dendrochronological reconstruction as aimed in this study requires methods other than usually applied in determining thresholds of landslide activity. Therefore, our methodological approach is based on previous studies by Papciak et al. (2015) and Wistuba et al. (2018, 2021), who showed that in analyses of landslide causes, the effects of uncertainty of dendrochronological dating can be reduced through extensive statistical analysis of various precipitation types and parameters.

2. Materials and methods

2.1. The study landslide

The Karpenciny landslide is located in the Central Western

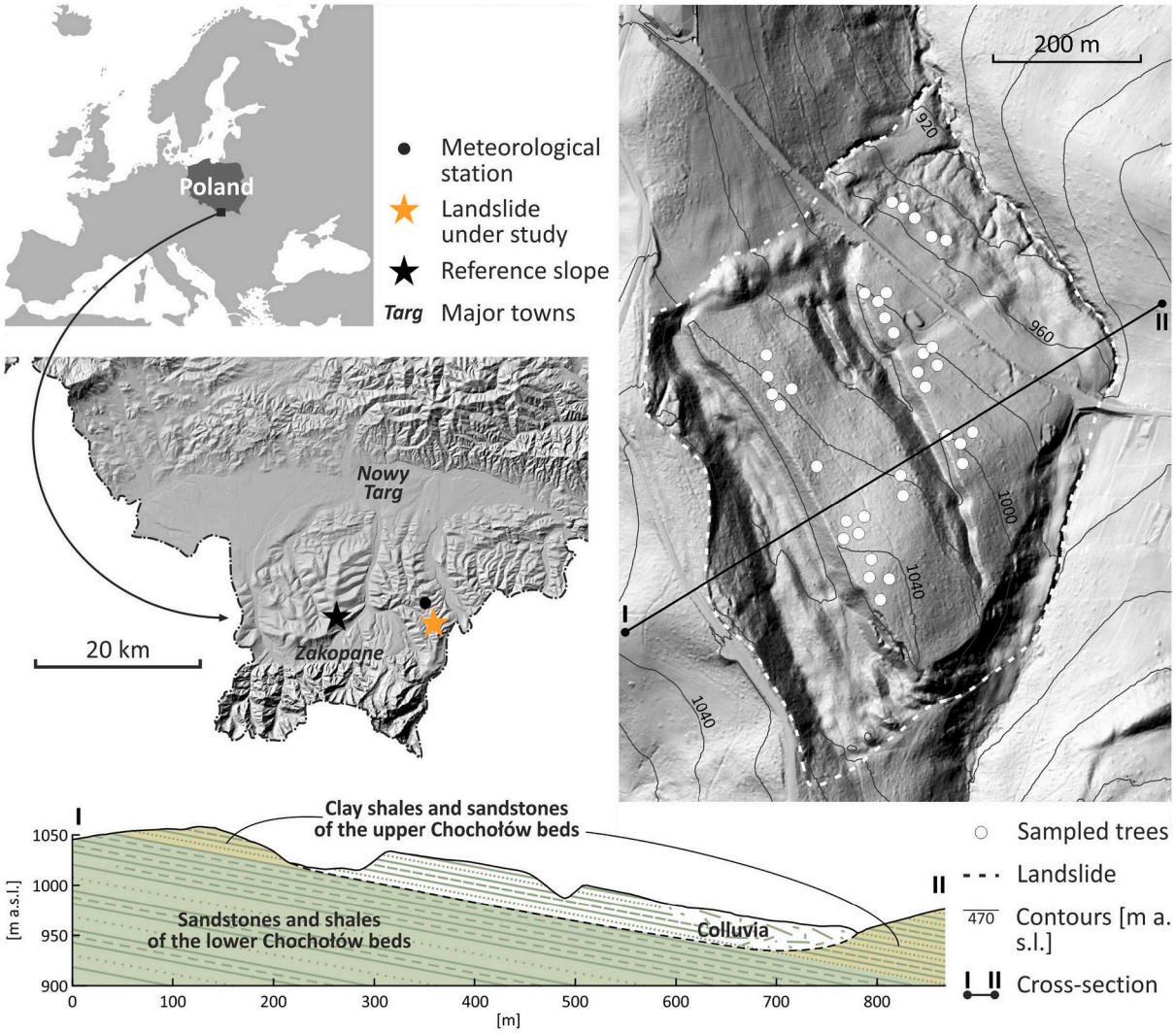

Fig. 2. Location of the Karpenciny landslide and the Białka Tatrzańska meteorological station in the Western Carpathians, Southern Poland. Topography and slope profile of the study landslide with the location of trees sampled for dendrochronological analysis (LiDAR data for digital terrain models obtained from the Central Agency of Geodetic and Cartographic Documentation CODGiK, Poland; and bedrock structure data from Piotrowska et al., 2017).

Carpathian Mountains, Southern Poland (49.32° N, 20.11° E) (Fig. 2), in a low mountainous region (less than 1200 m a.s.l., relief up to 550 m) where the slopes are usually less than 35° and 2 km (Długosz, 2011). The bedrock of the Eocene-Oligocene deposits of the flysch Podhale Basin (Fig. 2) often have bedding parallel to hillslopes, increasing their vulnerability to translational landslide movements which are enhanced by the thick shale layers acting as potential shear zones (Marciniec et al., 2019).

The studied landslide is typical of these geological settings. It is a vast (area: 37.4 ha, maximum length: 659.5 m, maximum width: 689.0 m) and deep (approximately 40 m), structural, translational rock-debris slide with poor fragmentation of landslide masses (Fig. 2). The landslide consists of large, almost intact landslide blocks divided by deep and long trenches (Fig. 2). The average slope of the landslide surface is 13.2°, and its relative height is 154.1 m (909.4–1063.5 m a.s.l.). In the Köppen–Geiger classification system, the study area has a humid continental climate of the warm summer subtype. The annual precipitation at Bukowina Tatrzańska gauge adjacent to the Karpenciny landslide (Fig. 2) ranges from 619.7 to 1362.6 mm, with an average total of 899.4 mm (1971–2019). Most of the precipitation occurs during the summer seasons, and the maximum daily precipitation is related to June–July cyclones with up to 100 mm of rainfall (11% of annual total) per 24 h. The mean monthly precipitation sums of the two months with the highest rainfall are 130 mm in June and 149 mm in July. In general, 55% of the annual precipitation occurs from May to August. Precipitation patterns are considerably consistent over the study area: mutual correlations between daily precipitation records (24-h precipitation totals during the entire observation periods) commonly exceed 0.8, for example, it was 0.86 for the Bukowina Tatrzańska and Zakopane station (11 km south-west from Bukowina Tatrzańska) (Wistuba et al., 2021). High correlation levels between the precipitation records of particular stations indicate substantially homogeneous precipitation over the study area. The average annual temperature in the area is 4–6 °C, and the snow cover lasts for 125–175 days annually (Cebulak, 1998).

2.2. Dendrochronological reconstruction of landslide activity

Dendrochronological reconstruction of the activity of the Karpenciny landslide was based on samples collected in late 2018 from 35 Norway spruce trees (*Picea abies*) (Fig. 2). We sampled all mature spruce trees which grew on the low-inclined, top surfaces of landslide blocks and were visually assessed as healthy and uninjured. Moreover, ten spruce trees were sampled on a reference slope (Fig. 2: 12 km west from the Karpenciny landslide, 49.32° N, 19.94° E), which does not show any landslide symptoms in its relief but presents similar inclination, aspect, altitude, and bedrock as the landslide under study. We used Pressler borers to collect samples, that is, increment cores from tree stems, and collected two cores from each tree: one from the upslope side and one

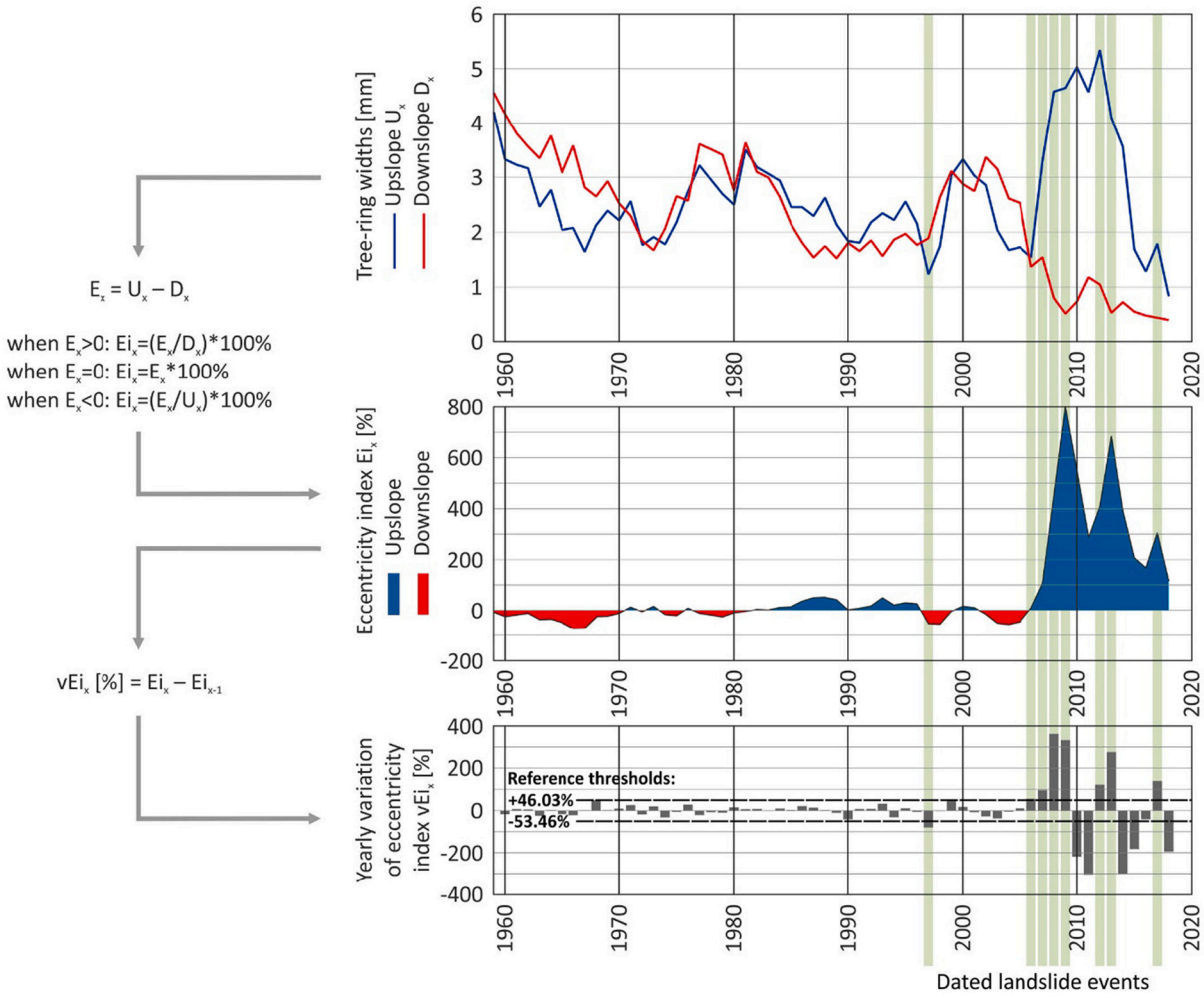

Fig. 3. Dating landslide activity from ring eccentricity in a single tree sampled on the Karpenciny landslide. Tree-ring widths are recalculated to obtain an eccentricity index and its yearly variation using the calculation by Wistuba et al. (2013): U – width of a tree ring in the upslope part of the stem [mm]; D – width of a tree ring in the downslope part of the stem [mm]; E – eccentricity of a tree ring [mm]; Ei – eccentricity index of a tree ring [%]; vEi – yearly variation of eccentricity index [%]; and x – year (annual tree ring).

from the downslope side of the stem, both at breast height. The cores were mounted on wooden laths and sanded to reveal the wood structure. The skeleton plot technique (Cropper, 1979) was used to cross-date between upslope and downslope samples of every tree to detect wedging rings and ensure correct dating results.

The wood anatomy in each single tree ring of each sample was analysed to identify compression wood, that is wood with intracellular spaces, thicker and more rounded cell walls, and smaller cell lumens (Ruelle, 2014) (Fig. 1). We used the criteria of Yumoto et al. (1983) to identify the compression wood, but avoided its gradation. However, we dated the oldest ring in each set of compression wood to determine the most probable time for landslides which disturbed stem stability.

To analyse eccentric tree rings (wider on one side of the tree stem: Fig. 1), we measured the widths of all rings in the samples from the landslide and reference slope (LinTAB measuring system, 0.01 mm accuracy). We recalculated the tree-ring widths on the upslope and downslope sides of each stem to obtain the eccentricity index and its annual variation (Malik and Wistuba, 2012; Wistuba et al., 2013) (Fig. 3). Annual variation is calculated to eliminate the effect of compensation which may occur in years following stem tilting (Wistuba et al., 2015). In this study, values of yearly variation obtained for all rings in ten reference trees were used to establish reference thresholds for dating landslide activity from the eccentricity record following the method by Malik and Wistuba (2012) and Wistuba et al. (2013). Reference thresholds were calculated as the sum of the average and standard deviation, separately for sets of all positive (as a threshold for upslope eccentricity: +46.03%) and negative (as a threshold for downslope eccentricity: −53.46%) variation values in reference trees. In the landslide slope samples, only the years in which variation values exceeded reference thresholds were considered as events of landslide activity (Fig. 3) (Wistuba et al., 2013).

Then, we calculated the total number of trees annually disturbed by the landslide activity. If both eccentricity and reaction wood were dated in the same tree ring, we recognised them as one event, and not two separate events in a year. We also calculated the response index as the percentage of trees disturbed by landslide activity each year in proportion to the sample depth value (the total number of sampled trees growing in the same year) (Shroder Jr., 1978) (Fig. 4). We considered the response index as a proxy for the level of activity of the Karpenciny landslide. We also determined specific events of increased landslide activity at Karpenciny as years when the response index values increased (compared to a previous year) and exceeded the average value of the response index for the period under analysis. This way, we refer to the aim of this study and emphasise years when landslide activity has begun, that is, years when the landslide was reactivated after periods of relative stability.

2.3. *Determining meteorological causes of landslide activity from dendrochronological data*

According to Poprawa and Rączkowski (2003), Rączkowski (2014), and Wistuba et al. (2018), landslide activity in the study area could have been caused by earthquakes and precipitation. However, Wistuba et al. (2021) suggests that compared to the significant impact of precipitation, seismic activity plays a minor role in the specific case of the Karpenciny landslide. Therefore, in this study, we compared the dendrochronological record of landslide activity at Karpenciny with precipitation at the closest gauging station in Bukowina Tatrzańska (Fig. 2: 2.4 km northwest from the landslide, 49.34° N, 20.10° E, elevation 904 m a.s.l.). Daily precipitation totals at the station are available from 01.01.1971 (Institute of Meteorology and Water Management, Poland). Thus, a detailed analysis of meteorological causes for the Karpenciny landslide covered 48 years, from 1971 to 2018, when the trees were sampled. During this period, the sample depth in the analysed population of trees

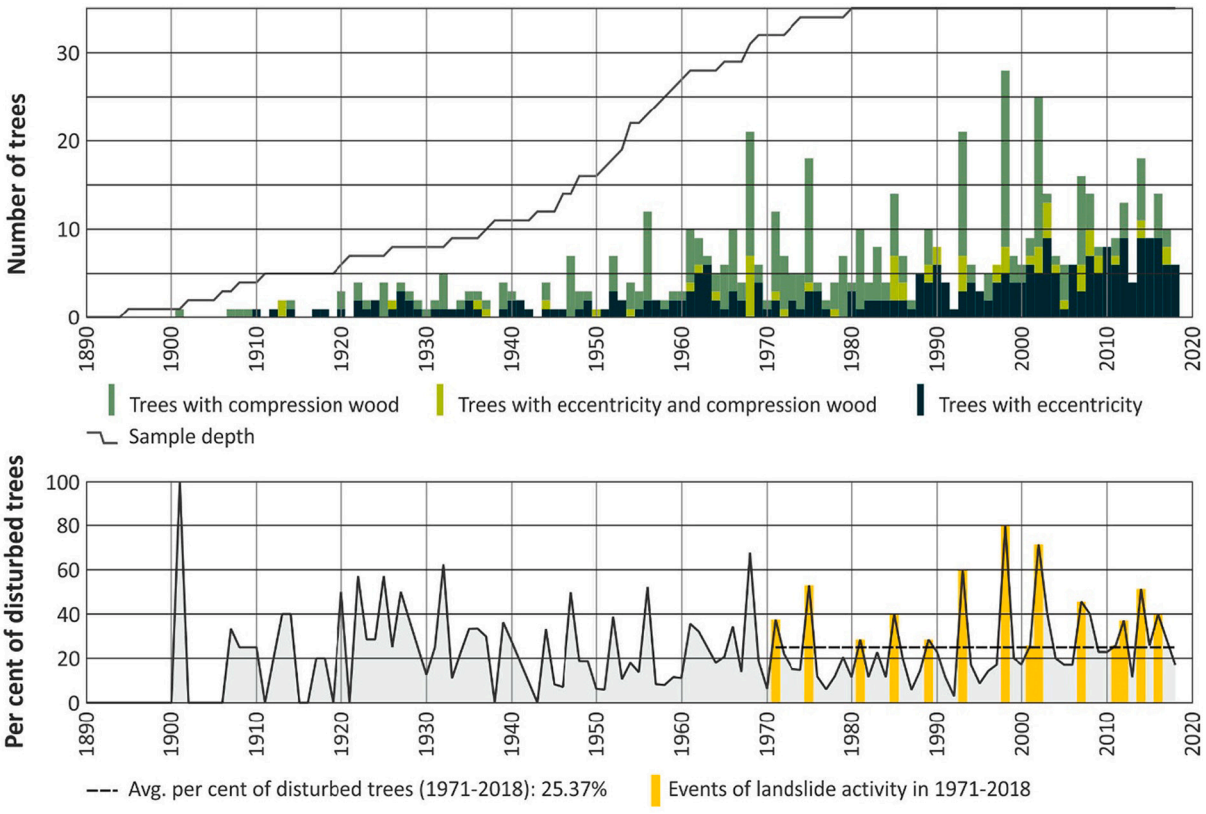

Fig. 4. Activity of the Karpenciny landslide reconstructed from tree rings. The number of trees with eccentricity and compression wood were compared to the sample depth and recalculated into response index values (% of disturbed trees in the sampled population).

was not less than 91.4% (32 of 35 trees) (Fig. 4).

We recalculated the daily precipitation totals into precipitation parameters for individual months (previous October, i.e. October of the year preceding calendar year with dated landslide activity, to present December, i.e. December of present calendar year with dated landslide activity) and longer seasons or periods (6 months of summer half-year: present April to present September, 6 months of preceding winter half-year: previous October to present March, 12 months of present summer half-year and preceding winter half-year: previous October to present September, 18 months of present summer half-year and preceding winter and summer half-years, 24 months of present summer half-year and preceding winter, summer and winter half-years). We included the following parameters for each monthly and 6–24-month period (total 520 parameters):

- precipitation total (mm),
- maximum 24-h precipitation total (mm),
- maximum and minimum 3-day, 5-day, 7-day, 10-day, 20-day, 30-day, 60-day, and 90-day moving totals of precipitation (mm),
- total number of days with precipitation (days),
- maximum period with daily precipitation (days),
- number of events with daily precipitation lasting 6–10, 11–15, 16–20, and $>$ 20 days in a row (events),
- number of days with precipitation of 30–50 and $>$ 50 mm per 24 h (days).

These listed precipitation datasets were statistically correlated with dendrochronological records of landslide activity. The statistical significance of the correlations was tested for $\alpha = 0.1$ and $\alpha = 0.05$, to determine the general, long-term relationship between landslides and precipitation. Ten parameters showing the highest positive correlation levels and three basic seasonal precipitation sums (preceding winter half-year, present summer half-year separately, and as 12 months in total) were used in further analysis of factors causing landslide reactivation. We searched for similarities between the temporal variability of these parameters and the tree-ring record of landslide activity: response index values and dated landslide events. In addition, we analysed events of landslide activity determined by Wistuba et al. (2021) on two other slopes in the study area (13 and 20 km west of Karpenciny). We compared the precipitation records for years when landslide events occurred at Karpenciny and years when events only occurred at two adjacent landslides. Thus, we aimed to determine whether any local site-specific causes occur only in the Karpenciny landslide.

2.4. Determining rainfall thresholds of landslide activity from dendrochronological data

We established rainfall thresholds for events of landslide activity at Karpenciny based on single precipitation parameters (assuming that the activity of the studied landslide can be explained with only one type of precipitation which is sufficient as a cause of landslide reactivation). Therefore, for each of the 13 selected parameters (10 best-correlated and three basic seasonal sums as previously mentioned), we prepared a scatter plot for the 48-y study period (1971–2018), with values of response index on the X-axis and values of specific precipitation parameter on the Y-axis. We divided the data presented on all plots into years with and without landslide events (determined as described previously). We checked for the highest levels of precipitation parameters, below which no landslide event was recorded at Karpenciny and for the lowest levels of precipitation, above which only landslide events occurred. We also checked for the highest levels of precipitation above which the number of years with events exceeded the number of years without events; therefore, the probability of the occurrence of a landslide event exceeded 0.5. We ensured that all established thresholds separated at least two data points from the rest of the dataset.

We also established rainfall thresholds for events of landslide activity at Karpenciny based on pairs of precipitation parameters (assuming that the studied landslide activity can be explained by two types of precipitation, both necessary for landslide events). Therefore, we prepared scatter plots based on the pairs of values of precipitation parameters for all years in the 48-y study period (1971–2018). We combined the 13 selected parameters with each other in a matrix of 78 plots. Then, we divided the presented data into years with and without landslide events and checked all plots for the two types of threshold lines:

- upper threshold line separating precipitation conditions which were always in the past (in the studied period) associated with landslide events, from conditions which were or were not associated with landslide events;
- lower threshold line separating precipitation conditions which were never in the past (in the studied period) associated with landslide events, from conditions which were or were not associated with landslide events.

The two threshold lines would divide the area of a scatter plot into three parts: upper, where there are only years with dated landslide events; lower, where there are only years without dated landslide events; and middle, where years with and without dated events merge. The thresholds were determined manually, following the same procedure for all plots. All thresholds were drawn as straight lines dividing the above-mentioned parts of the plots (parts of datasets) in the middle between their outermost data points. We ensured that the thresholds separated as many years with and without events as possible (by upper and lower thresholds, respectively), but not less than two data points per threshold line. Threshold lines represent the assumption that an increase in precipitation parameters causes an increase in landslide activity. Thus, lines were only drawn from top left to bottom right (indicating that both parameters affect landslide activity), vertically and horizontally (indicating that only one of the two parameters affects landslide activity). Priority has been given for threshold lines fitting all data presented on particular plots (called complete threshold lines) over those fitting only parts of datasets (called incomplete threshold lines).

Then, we checked the efficiency of the thresholds provided by each of the 78 pairs of precipitation parameters. We checked the number of years with events separated by each upper threshold line and those without events separated by each lower threshold line, and selected ten best-performing pairs of precipitation parameters as those providing two complete thresholds (upper and lower) that separated the highest number of years. Furthermore, we omitted pairs of parameters (even those showing good efficiency in separating data points) which provide only one threshold (upper or lower), horizontal and vertical thresholds, incomplete thresholds, or two equally effective potential threshold lines.

3. Results

3.1. Relationship between the activity of the Karpenciny landslide and different types of precipitation during 1971–2018

Positive and statistically significant correlations of precipitation parameters and response index values (Fig. 4) were strongly clustered in particular seasons and months (Table A.1). This indicates that the activity of the Karpenciny landslide has a clear relationship with meteorological causes, mostly with minimum totals of the previous October, maximum totals of February, and various parameters for the present October. Significant positive correlations were also obtained for the number of daily precipitation events lasting 11–15 days in June and previous November and for long-term maximum totals during 12–24 months (Table A.1). Therefore, these types of precipitation were the most probable causes of landslide activity at Karpenciny. The ten highest correlation coefficients (Table 1: 0.31–0.45) were all statistically significant for $\alpha = 0.05$ (Table A.1). Moreover, the correlation levels for the three basic seasonal precipitation sums were lower (Table 1: 0.14–0.19)

Table 1
Comparison between the thirteen selected precipitation parameters and tree-ring record of landslide activity at Karpenciny (response index values): correlation coefficients, similarity (% of 1971–2018 period with identical and simultaneous changes, increases and decreases, in landslide activity and precipitation) and simultaneous increases of precipitation and landslide activity (% of all increases of precipitation level).

Precipitation parameters: the 10 best-correlated with landslide (Table A.1) and three seasonal sums	Correlation coefficient	Similarity [% of time]	Simultaneous increases [% of all increases]
Minimum 7-day total in previous October*	0.45	30.43	54.55
Number of events with daily precipitation lasting 11–15 days in June*	0.40	27.66	75.00
Total number of days with precipitation in October*	0.39	68.09	66.67
Minimum 30-day total in October*	0.39	63.83	61.11
Maximum 24-h total in February*	0.35	44.68	37.50
Maximum 60-day total during 24 months of present summer half-year and preceding winter, summer and winter half-years*	0.34	31.91	50.00
Maximum 5-day total in October*	0.33	61.70	54.17
Minimum 10-day total in previous October*	0.32	41.30	45.00
Minimum 20-day total in previous October*	0.31	47.83	36.84
Number of events with daily precipitation lasting 6–10 days in October*	0.31	40.43	50.00
Sum for 6 months of preceding winter half-year (previous October to present March)**	0.14	46.81	40.00
Sum for 6 months of present summer half-year (present April to present September)**	0.15	53.19	45.45
Sum for 12 months of present summer half-year and preceding winter half-year in total (previous October to present September)**	0.19	63.04	56.52

* The ten precipitation parameters best-correlated with landslide activity.
** Three seasonal sums.

and were all statistically insignificant for $\alpha = 0.05$ and $\alpha = 0.1$ (Table A.1).

Among the 13 parameters selected for further analysis, the highest correlation values and the highest levels of similarity between increases and decreases were found for: minimum 7-day total in previous October, number of events with daily precipitation lasting 11–15 days in June, the total number of days with precipitation, minimum 30-day total and maximum 5-day total in October, and a 12-month sum of the present summer half-year and preceding winter half-year in total (previous October to present September) (Table 1). The results reveal the highest dependence of landslide activity from these six precipitation parameters and the highest probability that an increase in these precipitation types will accelerate landslide activity (Table 1: >50% of increases in this types of precipitation during 1971–2018 is related to the simultaneous increase in landslide activity). However, the similarity between precipitation and landslide activity changed over time. There were periods of complete similarity and periods of complete divergence (Figs. 5 and 6). This showed that even though the analysed types of precipitation could influence landslide activity at Karpenciny over longer periods of several years, none alone could completely control it during the entire study period.

Fourteen landslide events were dated from 1971 to 2018 at the Karpenciny landslide based on the average value of the response index (Fig. 4). Nine of the events found by Wistuba et al. (2021) on other landslides in the study area were not dated at Karpenciny. Two of these events (1979 and 1983) were slightly marked in the data for the Karpenciny landslide but without the response index exceeding its average for 1971–2018 (Figs. 4–6). However, the similarity between the dendrochronological record of the activity of the Karpenciny landslide and other landslides in the study area was high, based on both dated events and entire curves of reconstructed landslide activity (Wistuba et al., 2021). This indicates that the dated activity of the Karpenciny landslide is consistent with the regional trends of landslide activity in the study area.

The total number of days with precipitation and maximum 5-day total in October, and the 12-month sum of present summer half-year and preceding winter half-year in total are probably the most frequent causes of landslide events at Karpenciny. Increases in these parameters present the best direct similarity (69.2–76.9%) with dated events (Table 2). This percentage increased to 84.6–100% (Table 2) on including events that were lagging in relation to increases in: the maximum 5-day total, the total number of days with precipitation, and the number of events with daily precipitation lasting 6–10 days in October. Thus, simultaneous and prior increases in the three precipitation parameters explain the occurrence of all or almost all landslide activity events at Karpenciny (Fig. 5). However, among the increases in precipitation that are similar to the events, there were extreme events that might cause landslide activity and slight changes, which may be too weak to cause reactivations. Their coincidence with landslide events was considered to be random (Fig. 5, Tables B.1 and B.2).

Only 20–40% of events absent at Karpenciny but reported by Wistuba et al. (2021) on adjacent slopes precisely corresponded with increases in single precipitation parameters under analysis (Table 3). This suggests significant differences in the reactivation causes between Karpenciny and other landslides in the study area. Even including the lagged impact of precipitation on landslide activity (Table 3) does not increase the percentage of similar events for the following three precipitation parameters: the number of events with daily precipitation lasting 11–15 days in June (one matching event), minimum 7-day total in previous October (two matching events, including one nominal: Table B.3), and maximum 60-day total during 24 months of the present summer half-year and preceding winter, summer, and winter half-years (three matching events) (Table 3). Therefore, the three above-mentioned parameters are probably local, site-specific, and unique to Karpenciny. Increases in these parameters occurred for all landslide events dated at Karpenciny, except one (Table B.1). The remaining ten parameters represented regional causative factors that exert a more widespread impact on the slopes of the study area.

3.2. *Rainfall thresholds for Karpenciny landslide established from single precipitation parameters*

All types of precipitation selected for the analysis (the 10 best-correlated and three basic seasonal sums) showed a clear positive relationship with landslide activity.

We established the lowest levels of past precipitation for three of the 13 studied parameters that were always related to landslide events at Karpenciny (Figs. 7 and 8). They constituted simple threshold levels of high precipitation, which, in the past, certainly caused landslide events, if reached and exceeded. However, their efficiency was limited to two years, with events separated from the rest of the datasets. Thus, their reliability was small and lower than the more efficient thresholds established as the highest levels of precipitation that have never been related to landslide events at Karpenciny (Figs. 7 and 8). These lower thresholds were established for the five studied parameters and they

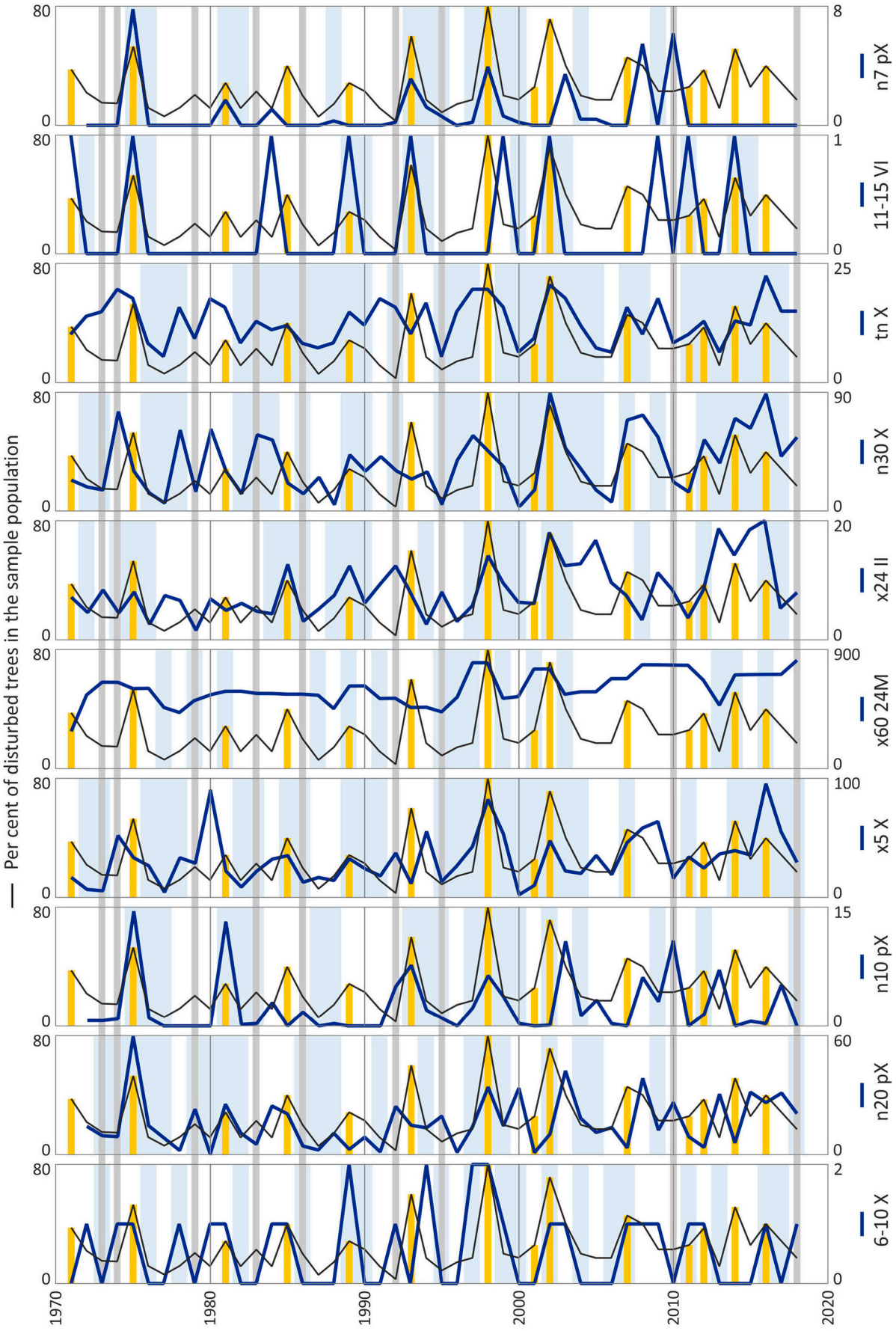

(caption on next page)

Fig. 5. Landslide activity (response index and dated events) for the Karpenciny site during 1971–2018 compared to the precipitation record (the ten best-correlated parameters according to Table A.1) (for legend see Fig. 6): n7 pX – minimum 7-day total in previous October [mm], 11–15 VI – number of events with daily precipitation lasting 11–15 days in June, tn X – total number of days with precipitation in October, n30 X – minimum 30-day total in October [mm], x24 II – maximum 24-h total in February [mm], x60 24 M – maximum 60-day total during 24 months of the present summer half-year and preceding winter, summer, and winter half-years [mm], x5 X – maximum 5-day total in October [mm], n10 pX – minimum 10-day total for previous October [mm], n20 pX – minimum 20-day total for previous October [mm], and 6–10 X – number of events with daily precipitation lasting 6–10 days in October.

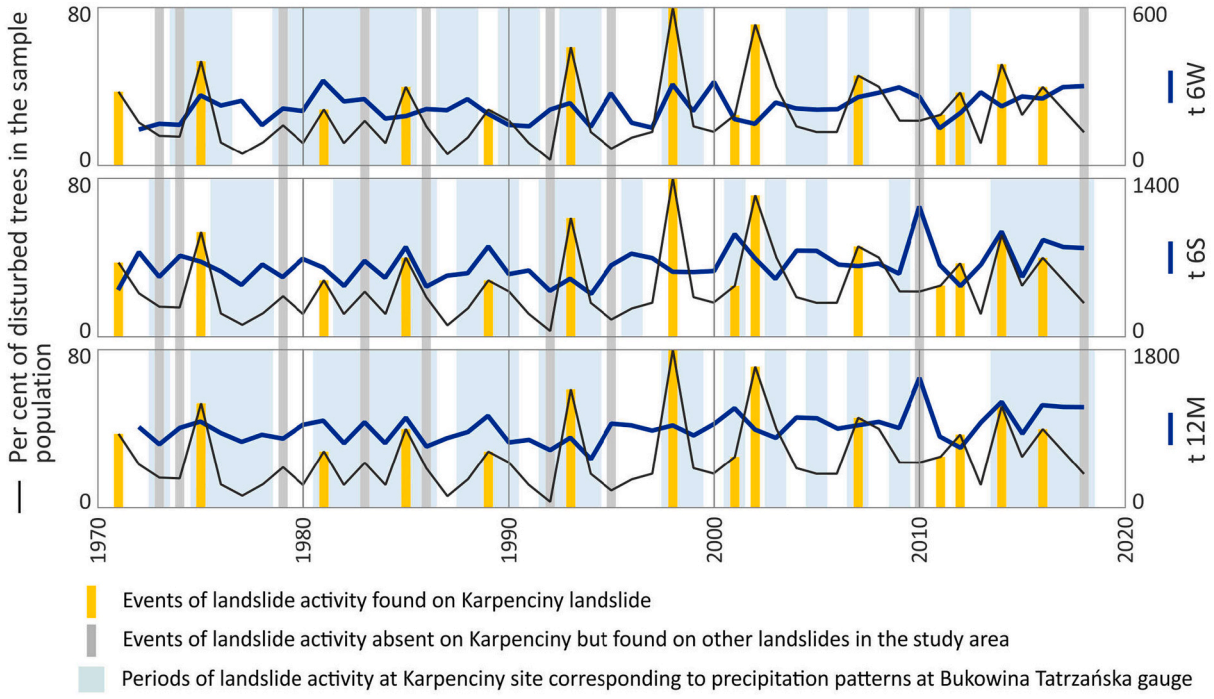

Fig. 6. Landslide activity (response index and dated events) for the Karpenciny site during 1971–2018 compared to the precipitation record (three seasonal sums): t 6 W – sum for 6 months of preceding winter half-year (previous October to present March) [mm], t 6S – sum for 6 months of present summer half-year (present April to present September) [mm], and t 12 M – 12-month sum of present summer half-year and preceding winter half-year in total (previous October to present September) [mm].

2–11 data points from the rest of the datasets. They comprised simple threshold levels of precipitation which were too low to ever cause landslide events. Therefore, these thresholds defined the upper boundary of landslide-safe conditions, such as a threshold of ≤9 days of precipitation occurring in total in October (based on 11 data points) and a ≤ 13.9 mm threshold for a minimum 30-day precipitation total in October (based on nine data points).

The precipitation levels were determined for 12 out of 13 precipitation parameters, above which the probability of a landslide event occurring at Karpenciny exceeds 0.5, based on up to 11 data points (Figs. 7 and 8). Exceeding these levels increases the probability of the occurrence of a landslide event over the probability of the absence of a landslide event, and the best-performing among those thresholds are:

- a threshold of 974.2 mm 12-month precipitation sum for present summer half-year and preceding winter half-year in total (which separated 11 data points),
- a threshold of 11–15 consecutive days with precipitation in June (10 data points; threshold based on simple zero-one occurrence or absence of a specific meteorological situation),
- a threshold of 774.1 mm for precipitation sum in 6 months of present summer half-year (nine data points),
- a threshold of 12.6 mm for a maximum 24-h total in February (nine data points).

3.3. Rainfall thresholds for Karpenciny landslide established from pairs of precipitation parameters

Among the 78 different pairs of precipitation parameters (scatter plots: Fig. C.1), 21 (Table D.1) pairs could be used to determine two complete precipitation thresholds (upper and lower) for the activity of the Karpenciny landslide, none of which was horizontal or vertical (thus suggesting that one of the precipitation parameters in the examined pair was suppressed by the other parameter and probably had no influence on the landslide activity), or ambiguous (with a potential for two equally efficient lines for one threshold) (Fig. C.1). The efficiency of thresholds established for these 21 pairs of precipitation parameters varied from 5 to 17 data points separated together by upper and lower thresholds, including 2–5 separated by the upper and 2–14 by the lower threshold lines (Table D.1). The disproportion between the efficiency of upper and lower thresholds indicates generally higher reliability of lower thresholds, which defines the upper boundary of precipitation conditions that were landslide-safe in the past. The reliability of upper thresholds constituting the lower boundary of precipitation conditions that always caused landslide events at Karpenciny was generally lower.

The ten best-performing pairs of precipitation parameters are shown in Fig. 9 and Table D.1, which included:

- seven pairs with the highest efficiency of both thresholds (14–17 separated data points), and at the same time the highest efficiency of lower threshold (11–14 separated data points) (Plots 14, 24–26, 33, 35, and 43),

Table 2
Similarity between increases in thirteen selected precipitation parameters and landslide events dated from tree rings at Karpenciny (based on Figs. 5 and 6, Tables B.1 and B.2).

Precipitation parameters: the 10 best-correlated with landslide (Table A.1) and three seasonal sums	Number of landslide activity events corresponding to increases of precipitation (% of 13[1] events)		
	Without a lag	With a lag[2]	Total
Minimum 7-day total in previous October*	4 (30.8)	-[3]	4 (30.8)
Number of events with daily precipitation lasting 11–15 days in June*	6 (46.2)	2 (15.4)	8 (61.2)
Total number of days with precipitation in October*	9 (69.2)	3 (23.1)	12 (92.3)
Minimum 30-day total in October*	7 (53.8)	3 (23.1)	10 (76.9)
Maximum 24-h total in February*	7 (53.8)	3 (23.1)	10 (76.9)
Maximum 60-day total during 24 months of present summer half-year and preceding winter, summer and winter half-years*	5 (38.5)	-[3]	5 (38.5)
Maximum 5-day total in October*	9 (69.2)	4 (30.8)	13 (100.0)
Minimum 10-day total in previous October*	6 (46.2)	-[3]	6 (46.2)
Minimum 20-day total in previous October*	5 (38.5)	-[3]	5 (38.5)
Number of events with daily precipitation lasting 6–10 days in October*	5 (38.5)	6 (46.2)	11 (84.6)
Sum for 6 months of preceding winter half-year (previous October to present March)**	7 (53.8)	-[3]	7 (53.8)
Sum for 6 months of present summer half-year (present April to present September)**	6 (46.2)	4 (30.8)	10 (76.9)
Sum for 12 months of present summer half-year and preceding winter half-year in total (previous October to present September)**	10 (76.9)	-[3]	10 (76.9)

* The ten precipitation parameters best-correlated with landslide activity.
** Three seasonal sums.
[1] 13 events were considered instead of all 14 dated events, as it was not possible to determine whether precipitation levels for the event in 1971 increased or decreased in relation to the previous year 1970 because precipitation in Bukowina Tatrzańska was measured only since 01.01.1971.
[2] Landslide activity events corresponding to increases in precipitation which occurred one year before or earlier than a year before, if the same increased level of precipitation lasted until the event.
[3] Lagged reaction of Karpenciny landslide to the increase in this parameter was not analysed as the parameter itself was already based on data from the previous year.

Table 3
Similarity between increases in thirteen selected precipitation parameters and landslide events found in the study area (according to Wistuba et al., 2021), but absent at Karpenciny (based on Figs. 5 and 6, Tables B.3 and B.4).

Precipitation parameters: the 10 best-correlated with landslide (Table A.1) and three seasonal sums	Events of landslide activity matching increases of precipitation: number (% of all nine events)		
	Without a lag	With a lag[1]	Total
Minimum 7-day total in previous October*	2 (22.2)	-[2]	2 (22.2)
Number of events with daily precipitation lasting 11–15 days in June*	0 (0.0)	1 (11.1)	1 (11.1)
Total number of days with precipitation in October*	3 (33.3)	5 (55.6)	8 (88.9)
Minimum 30-day total in October*	3 (33.3)	3 (33.3)	6 (66.7)
Maximum 24-h total in February*	4 (44.4)	4 (44.4)	8 (88.9)
Maximum 60-day total during 24 months of present summer half-year and preceding winter, summer and winter half-years*	3 (33.3)	-[2]	3 (33.3)
Maximum 5-day total in October*	3 (33.3)	4 (44.4)	7 (77.8)
Minimum 10-day total in previous October*	5 (55.6)	-[2]	5 (55.6)
Minimum 20-day total in previous October*	4 (44.4)	-[2]	4 (44.4)
Number of events with daily precipitation lasting 6–10 days in October*	3 (33.3)	5 (55.6)	8 (88.9)
Sum for 6 months of preceding winter half-year (previous October to present March)**	7 (77.8)	-[2]	7 (77.8)
Sum for 6 months of present summer half-year (present April to present September)**	4 (44.4)	4 (44.4)	8 (88.9)
Sum for 12 months of present summer half-year and preceding winter half-year in total (previous October to present September)**	4 (44.4)	-[2]	4 (44.4)

* The ten precipitation parameters best-correlated with landslide activity.
** Three seasonal sums.
[1] Landslide activity events corresponding to increases in precipitation which occurred one year before or earlier than a year before, if the same increased level of precipitation lasted until the event.
[2] Lagged reaction of landslides to the increase in this parameter was not analysed as the parameter itself was already based on data from the previous year.

- three with the highest efficiency of upper thresholds (4–5 separated data points) (Plots 15, 22, and 47).

Eight out of the thirteen precipitation parameters analysed in detail constituted all pairs of parameters that provided the ten best-performing thresholds (Fig. 9: six among the best-correlated parameters, two among the basic seasonal sums). The total number of days with precipitation in October and maximum 24-h precipitation total in February were the most frequent among the best-performing thresholds (each parameter appears on four plots in Fig. 9). The former precipitation type was involved in the four most efficient pairs of parameters with 13–14 data points separated by lower thresholds and 15–17 by both thresholds in total (Table D.1).

Three precipitation parameters constituting the best-performing thresholds were involved in only one pair of parameters (scatter plots in Fig. 9). These parameters included two seasonal sums, which indicates that their potential for establishing thresholds of landslide activity at Karpenciny was significantly lower than the potential of best-correlated parameters.

The established threshold lines had diverse gradients (Fig. 9). The more horizontal or vertical these lines are, the more unbalanced the impact of the two involved precipitation parameters on landslide activity, that is, the more the dominating parameter suppressed the impact of the other. The upper and lower threshold lines established from one pair of precipitation parameters could also have diverse inclinations towards each other (Fig. 9). The more parallel they are, the more coherent the influence of the involved precipitation parameters on the Karpenciny landslide activity. The most coherent thresholds were determined from the minimum 30-day total in October paired with the total number of days with precipitation in October, as well as with a maximum 60-day total during 24 months of the present summer half-year and preceding winter, summer, and winter half-years (Fig. 9: Plots 24 and 35). The first of the above-mentioned pairs also presents a particularly balanced impact on landslide activity (Fig. 9: Plot 24).

4. Discussion

4.1. Precipitation controlling the activity of Karpenciny landslide over the past 60 years

Dendrochronological interpretation of the relationship between precipitation and any landslide activity can be aided by the knowledge of the duration of the growing and dormant seasons in a particular area. The growing season of Norway spruce on the upper timberline 9 km south-west of Karpenciny lasts from mid-May to the end of September (Kaczka et al., 2017). The Karpenciny landslide is located 400–600 m below the above-mentioned upper timberline of the study area. Thus,

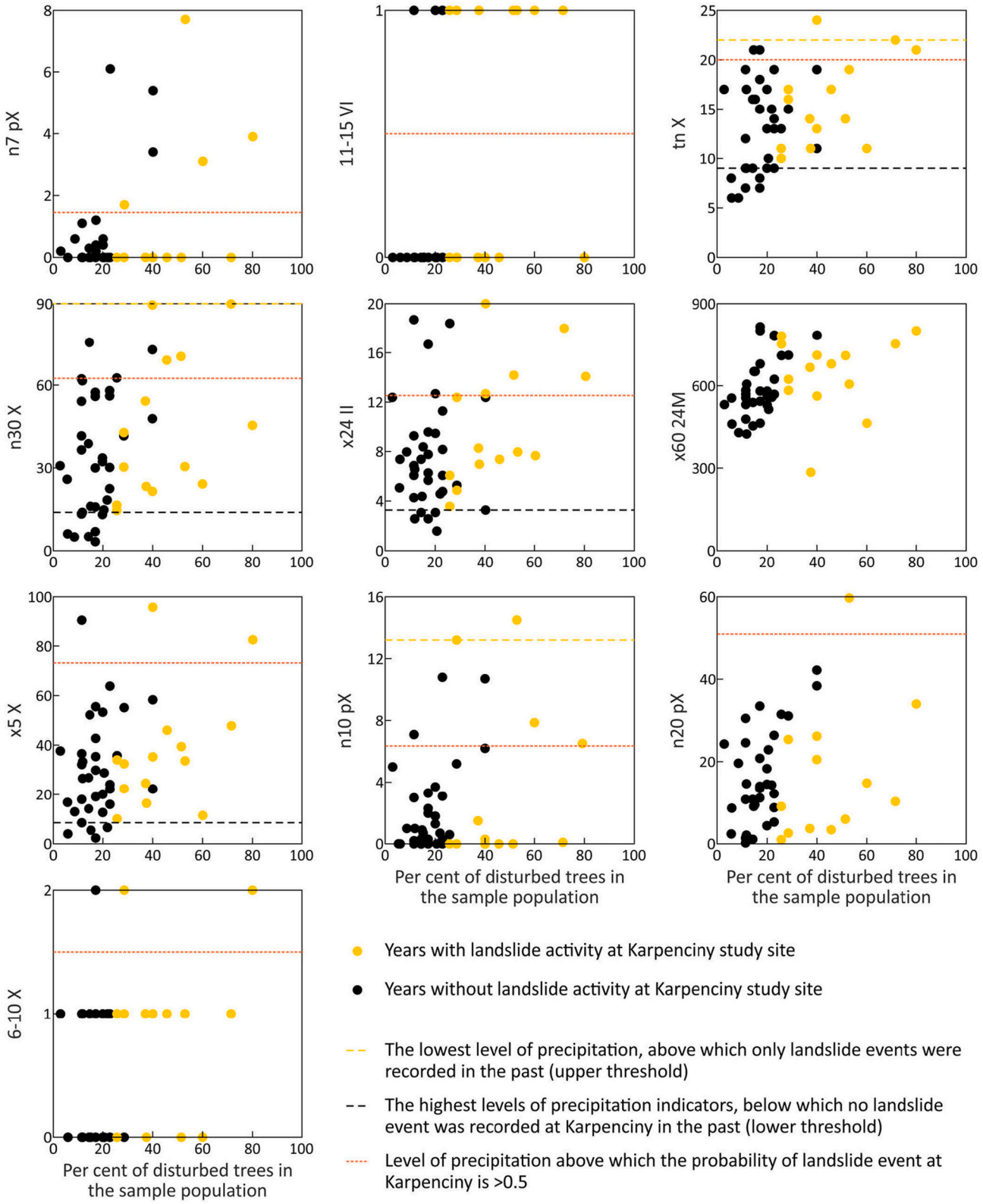

Fig. 7. Precipitation thresholds established as a representation of the relation between the activity of Karpenciny landslide (response index – % of disturbed trees in the sampled population) and individual precipitation parameters in this study (i.e. ten best-correlated parameters according to Table A.1) for each year during 1971–2018 presented on XY charts: n7 pX – minimum 7-day total in the previous October [mm], 11–15 VI – number of events with daily precipitation lasting 11–15 days in June, tn X – total number of days with precipitation in October, n30 X – minimum 30-day total in October [mm], x24 II – maximum 24-hour total in February [mm], x60 24 M – maximum 60-day total during 24 months of present summer half-year and preceding winter, summer and winter half-years [mm], x5 X – maximum 5-day total in October [mm], n10 pX – minimum 10-day total in previous October [mm], n20 pX – minimum 20-day total in previous October [mm], and 6–10 X – number of events with daily precipitation lasting 6–10 days in October.

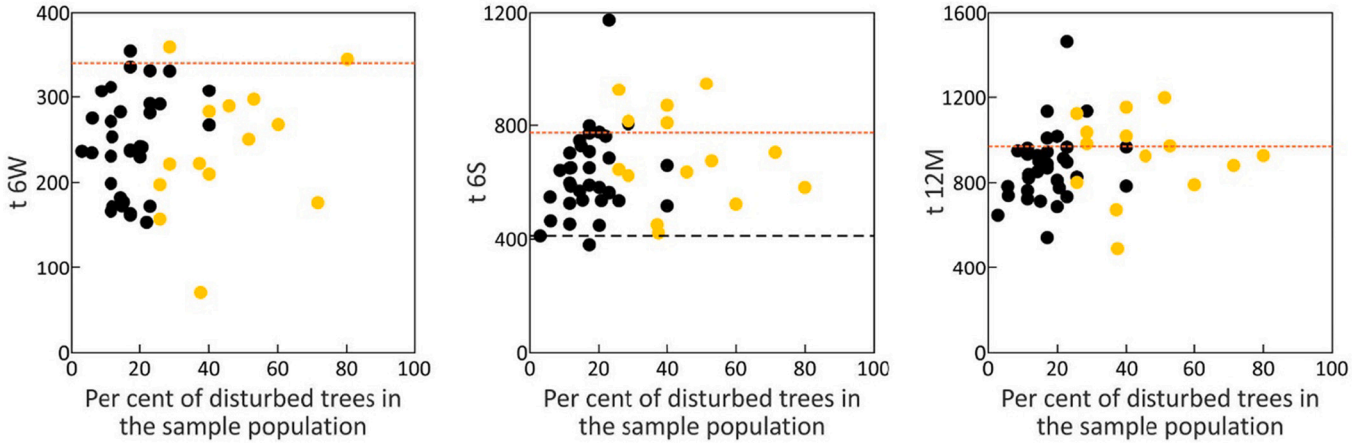

Fig. 8. Precipitation thresholds established as a representation of the relation between the activity of Karpenciny landslide (response index – % of disturbed trees in the sampled population) and individual precipitation parameters under study (i.e. three basic seasonal sums of precipitation) in each year during 1971–2018 presented on XY charts (for legend see Fig. 7): t 6 W – sum for 6 months of preceding winter half-year (previous October to present March) [mm], t 6S – sum for 6 months of present summer half-year (present April to present September) [mm], and t 12 M – sum for 12 months of present summer half-year and preceding winter half-year in total (previous October to present September) [mm].

the growing season for Norway spruces sampled in this study was assumed to last from April to October (Fig. 10). Moreover, recent research by Cabon et al. (2020) demonstrated that cambium activity and wood formation in coniferous trees in mountain habitats can last up to late autumn. Thus, each annual ring in samples from Karpenciny potentially records landslides from the preceding November to present October, that is, during the present growing season and preceding dormant season. Another important issue is the potential seasonality of landslide accelerations, which generally occur during summer in Polish Western Carpathians (Rączkowski, 2007). However, landslides in the study area (Central Western Carpathians) do not fit into this pattern (Rączkowski, 2014). There are inclinometer records of their accelerations in November–March (Państwowy Instytut Geologiczny, 2016), despite the domination of snowfall over rainfall in late autumn and winter and the lag between snowfall and actual delivery of melted water to the soil.

Thus, our results indicate that meteorological conditions, which generally favoured landslide activity at Karpenciny (Fig. 10) included long periods of preparatory precipitation, extending even before the preceding summer half-year, but certainly including directly preceding winter half-years (Fig. 10). This corresponds with existing knowledge on the dependence of landslide activity from long-term precipitation conditions of several months, seasons, or even years (Prokešová et al., 2012; Pennington et al., 2014). The results for Karpenciny are also consistent with the findings of Szabó (2003) on October precipitation, which significantly added to persistently high levels of groundwater in landslides in the Hungarian Carpathians, as well as with the findings of Arghiuş et al. (2011) from Romanian Carpathians, where landslide activity depends on snowmelt. The impact of autumn precipitation and spring thaw on the Karpenciny landslide is supported by the low evapotranspiration of these cool seasons (Błażejczyk, 2019), which facilitates a more efficient infiltration of water compared to summer seasons.

Spring thaw can also act as a direct cause of landslide activity (e.g. Chleborad, 1997; Cardinali et al., 2000), including the activity of the Karpenciny landslide (Fig. 10). Other direct causes can include the summer precipitation in June (Fig. 10), corresponding with the general information of landslide activity in the Polish Carpathians (e.g. Rączkowski, 2007; Gorczyca, 2010; Gorczyca et al., 2013). Landslide activity at Karpenciny can also be caused in late autumn by precipitation in October, similar to the landslides described by Jaedicke and Kleven (2008) and Brunetti et al. (2010).

Particular landslide events dated at Karpenciny might be related to more than one potential direct trigger (Fig. 10). This suggests that landslide activity at Karpenciny can be initiated by one of the determined causes (e.g. spring thaw or summer precipitation), continue in the following months, and be enhanced by other factors (e.g. summer and autumn precipitation). Similarly, Fiorucci et al. (2011) revealed that high landslide activity lasting from 2004 to 2005 in Italy was caused by consecutive diverse meteorological impulses, that is, rainfall events and rainy periods during September–June.

4.2. *Specific meteorological causes of landslide activity at Karpenciny and their potential in determining precipitation thresholds*

The results obtained for the Karpenciny landslide indicate that the precipitation parameters that are the best correlated and most similar to the dendrochronological record of landslide activity exhibit higher potential in establishing precipitation thresholds (Figs. 7–9), than the three seasonal sums, which have significantly lower correlations with landslide activity. The precipitation parameters that provide the best representation of local, site-specific causes of the studied landslide activity include daily precipitation lasting 11–15 days in June, minimum 7-day total in previous October, and maximum 60-day total during the 24-month preparatory period (Table 3). These parameters can be efficient in predicting landslide activity at Karpenciny as they correspond to all but one dated landslide event. Their absence clarifies why, even in wet conditions, when other landslides in the study area are active, the Karpenciny landslide remains inactive (e.g. 1995) or reactivates only slightly (e.g. 1983) (Figs. 5 and 6).

The results also show that minimum precipitation totals are often more important for the studied landslide than absolute or maximum totals. This is unexpected because numerous previous studies on precipitation thresholds attribute the causes of landslides to heavy precipitation events with extremely high intensities and totals (Govi and Sorzana, 1980; Zêzere, 2000; Garcia-Urquia, 2016; Yang et al., 2020). However, at Karpenciny favourable conditions for landslide acceleration can rather be ensured by precipitation not falling below a critical minimum level that is required to sustain the state of slope imbalance. A particular minimum amount of precipitation is required (and is sufficient) to cause the activity of the Karpenciny landslide. After this minimum amount of precipitation is exceeded, the final total precipitation becomes less important.

Our results also demonstrate that among the precipitation

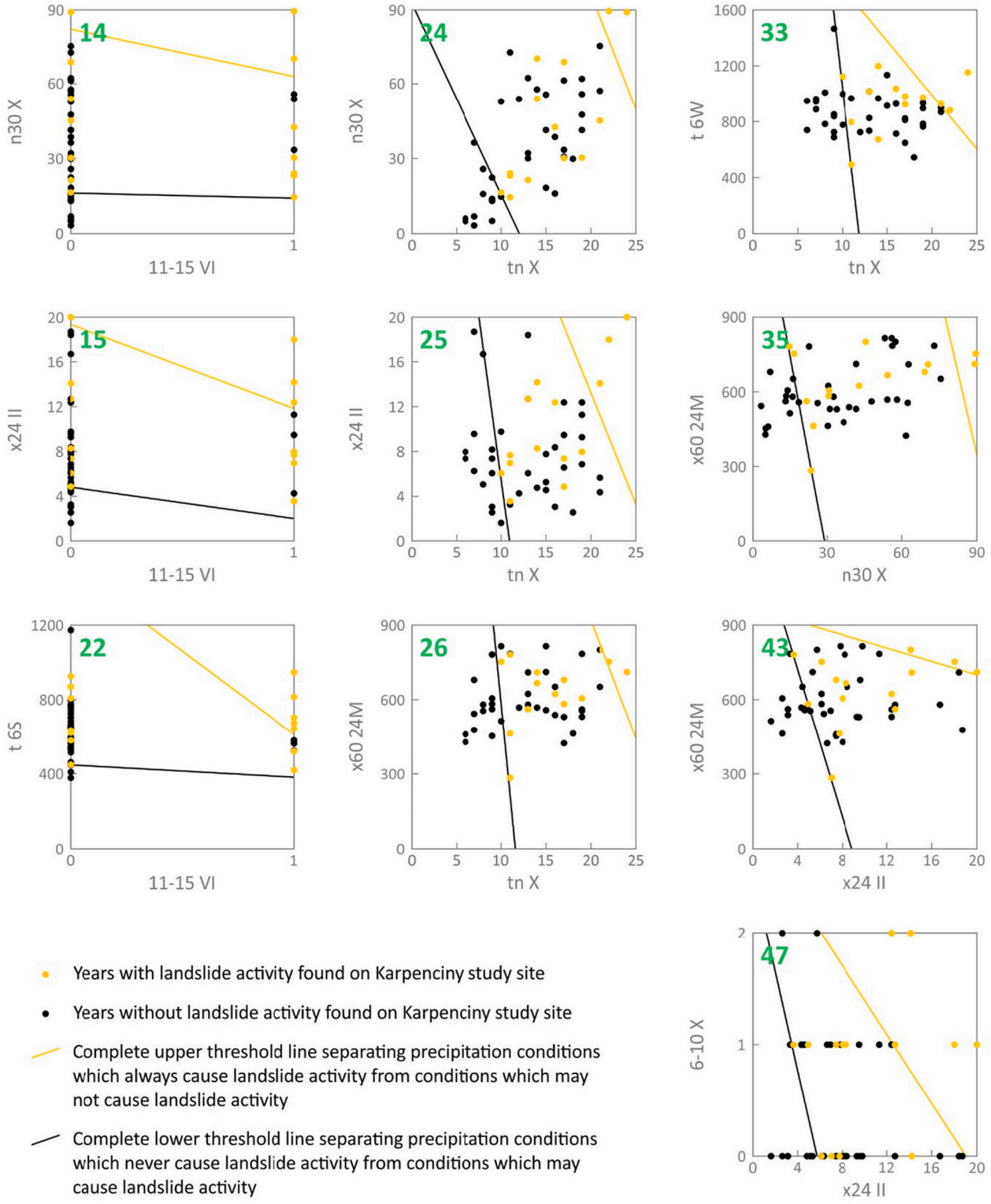

Fig. 9. Best-performing precipitation thresholds established as a representation of the relation between the activity of Karpenciny landslide (response index – % of disturbed trees in the sampled population) and pairs of precipitation parameters in each year during 1971–2018 presented on XY charts (selected from all examined pairs of parameters: Fig. C.1 and Table D.1): 11–15 VI – number of events with daily precipitation lasting 11–15 days in June, tn X – total number of days with precipitation in October, n30 X – minimum 30-day total in October [mm], x24 II – maximum 24-h total in February [mm], x60 24 M – maximum 60-day total during 24 months of present summer half-year and preceding winter, summer and winter half-years [mm], 6–10 X – number of events with daily precipitation lasting 6–10 days in October, t 6 W – sum for 6 months of preceding winter half-year (previous October to present March) [mm], and t 6S – sum for 6 months of present summer half-year (present April to present September) [mm].

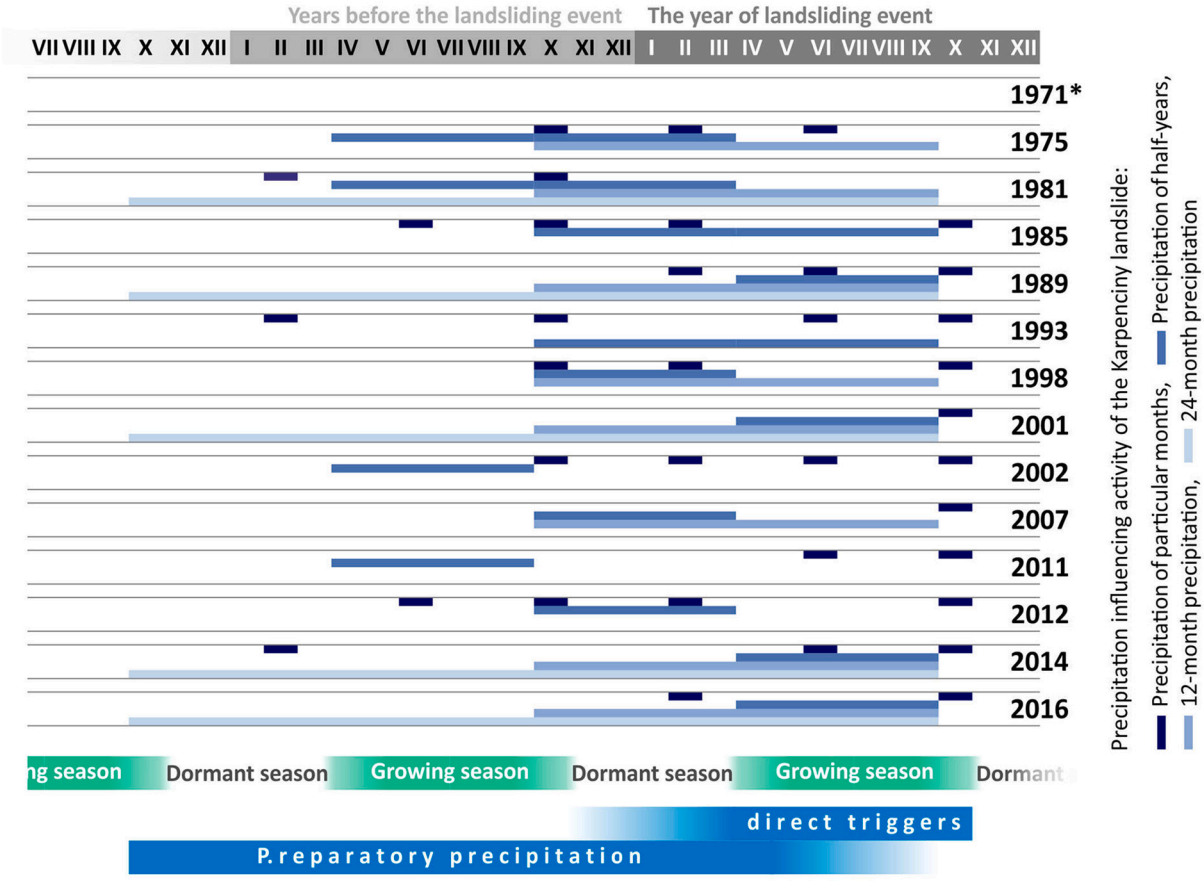

Fig. 10. Seasonality of precipitation affecting landslide activity at Karpenciny. Interpretation based on the dendrochronological reconstruction of landslides (1971, 1975, 1981, etc. – dated events), statistical analysis (ten best-correlated precipitation parameters and three seasonal parameters), duration of growing and dormant seasons and seasonality of landslide activity in the study area; * the event in 1971 could not be analysed because precipitation in Bukowina Tatrzańska was measured only since 01.01.1971, and no data from 1970 are available for comparisons (see Tables B.1 and B.2).

parameters crucial for the studied landslide, there are those based on the number of days with precipitation and the length of periods with daily precipitation (Tables A.1 and 1). This suggests that at Karpenciny, frequent and long-lasting precipitation can effectively cause landslide activity irrespective of the total of this precipitation. Such regularities are rarely reflected in previously reported rainfall thresholds. Although some of them include the potential importance of the length of rainfall, they are mostly focused on the duration and intensity (e.g. Zêzere, 2000; Hong et al., 2005) during hours and days directly before landslide events (Guzzetti et al., 2007; Segoni et al., 2018; Yang et al., 2020). Limited attention has been paid to antecedent precipitation over periods longer than a few weeks (e.g. Crozier, 1986; Glade, 2000; Segoni et al., 2014a, 2014b), with very few examples of thresholds including seasonal totals, such as rainfall totals for nine months of wet seasons analysed by Garland and Olivier (1993).

The critical minimum totals, seasonal antecedent precipitation, and generally wet conditions (demonstrated here as a high total number of days with precipitation) were proven to be essential for landslide activity at Karpenciny. However, they are not reflected by meteorological parameters usually included in precipitation thresholds, such as duration and intensity, precipitation sums (Govi and Sorzana, 1980; Bell and Maud, 2000; Zêzere, 2000) and averages (Caine, 1980; Brunetti et al., 2010), cumulated precipitation (Caine, 1980; Corominas and Moya, 1999; Bell and Maud, 2000), and normalised precipitation (Aleotti, 2004; Martelloni et al., 2012). Our results suggest that nonstandard parameters of precipitation, such as the above-mentioned parameters determined for Karpenciny, could be included in determining thresholds of landslide activity with methods other than dendrochronology, which might improve the efficiency of those thresholds.

Preparatory antecedent precipitation, occurring with a large advance before a landslide event (as demonstrated for Karpenciny), has a particularly high potential for practical applications in hazard analyses. Thresholds based on a combination of direct triggers (at Karpenciny, e.g. events with daily precipitation lasting 11–15 days in June and parameters of present October: Table 1) and antecedent precipitation of preceding 6–24 months (at Karpenciny, e.g. maximum 24-h total in February, minimum totals in previous October, and maximum 60-day total during 24 months) (Fig. 9) should be useful in early warning against landslide acceleration. The antecedent preparatory precipitation can be monitored in advance and used as an early sign of potential landslide reactivation. An exceeded critical level of antecedent precipitation would indicate that any further meteorological monitoring should focus on the possible occurrence of a certain direct trigger included in the threshold.

Although the dendrochronological approach can derive new data on landslide activity, it is affected by the annual resolution of tree-ring records. The latter results in uncertainty regarding specific dates of events and consequent differences between meteorological parameters usually applied in the analysed thresholds and parameters which were applied in this dendrochronological study. These differences prevent direct comparisons of thresholds obtained for Karpenciny (Figs. 7-9) with precipitation thresholds previously published for other landslides.

Some precipitation parameters were also indicated as causes of landslide activity at Karpenciny based on their high correlations with dendrochronological records; however, from a geological and geomorphological perspective, they cannot themselves effectively affect the

studied landslide. This includes short-term (including 24-h) precipitation in February, which is mainly snowfall in the studied area (Błażejczyk, 2019). Its impact on landslide activity is delayed until the spring thaw; thus, the total precipitation of particular days in February are in fact unimportant. However, such meteorological parameters appear to be the best statistical representation of the general importance of heavy snowfall at the turn of winter and spring, directly before or even at the beginning of the thaw period. Moreover, the high correlation of the discussed precipitation parameter with landslides at Karpenciny makes it valuable for determining threshold levels.

4.3. The potential of precipitation thresholds determined from long-term reconstructions of landslide activity

In the case of thresholds based on individual precipitation parameters (Figs. 7 and 8) and thresholds based on pairs of parameters (Figs. C.1 and 9), we found it easier and more frequently possible to determine lower threshold lines (separating precipitation conditions which were never related to landslide events in the past) than upper threshold lines (separating precipitation conditions which were always related to landslide events in the past). Established upper thresholds of precipitation are also less reliable, that is, based on a smaller number of data points than the lower thresholds. This is because even though the studied period of 1971–2018 covers almost 50 years, the number of landslide events dated on one studied slope remains lower (14) than the years without events (34). Nevertheless, the idea of determining three levels of precipitation that never, sometimes, and always caused landslide activity has great practical potential in hazard assessment. This is similar to the threshold levels previously established by Govi and Sorzana (1980), Glade (2000), and Bíl et al. (2016), who also included precipitation levels that never and always cause landslides. This preliminary research indicates that dendrochronology can at least help to determine precipitation conditions that are landslide-safe and never caused landslide events in the past. Tree rings can also be an efficient source of data on levels of precipitation above which landslide acceleration is more probable than maintaining slope stability (Figs. 7 and 8), similar to probability-based precipitation thresholds for landslides established by among all Berti et al. (2012) and Zhao et al. (2019). However, the annual (rarely sub-annual) resolution of dendrochronological dating, which prevents identification of the exact timing and causes of landslide activity, is an unavoidable limitation in the practical application of precipitation thresholds derived from tree-ring data.

Generally, thresholds determined from comparisons of tree-ring response index with single precipitation parameters (Figs. 7 and 8) are a better representation of the relationships between precipitation and diverse levels of landslide activity. In contrast, thresholds based on pairs of parameters can provide better performance (Figs. 7–9 and Table D.1). However, despite the high correlations between the studied precipitation parameters and landslide records, only 27% of the examined pairs of parameters meet the assumed primary conditions. These pairs provide both upper and lower threshold lines, none of which are horizontal, vertical, or incomplete, or can be drawn in two equally effective ways. Many examined pairs of precipitation parameters only allowed the establishment of threshold lines with the above-mentioned flaws, lines that are strongly oblique or even intersect one another. This suggests that curved threshold lines should be determined, except for straight ones in such cases. The latter is a simplification, assuming proportional, linear relations between increases in precipitation and landslide activity. However, after precipitation exceeds a certain level, its further increase might have a larger or smaller impact on landslides than before, which can be reflected in precipitation thresholds established as curved lines (e.g. Crosta and Frattini, 2001; Garcia-Urquia, 2016). The issue of straight threshold lines is evident for precipitation parameters that can only have integral values, particularly parameters such as the number of events with daily precipitation lasting several days (Table 1, Figs. 5 and 6). If those threshold lines are established following the same rules as other parameters, they may adopt artificial, unrealistic values, for example, a threshold of 1.5 established for the number of events with daily precipitation lasting 6–10 days in October (Fig. 7). This particularly concerns thresholds established from pairs of precipitation parameters. In future research, this could be solved by establishing thresholds as steplike and broken lines, similar to some previous studies (e.g., Guzzetti et al., 2008; He et al., 2020).

Precipitation thresholds established from dendrochronological data also have limitations similar to those established from other data. In the case of the studied slope at Karpenciny, the first issue is the general difficulty of establishing precipitation thresholds for deep-seated landslides. Unlike shallow landslides triggered by intense short-duration rainfall, deep-seated landslides respond to long-term rainfall with high and medium intensity (Guzzetti et al., 2007; Segoni et al., 2014a, 2014b). Reactivation of a deep-seated landslide is considered a complex process (Zhang et al., 2006; Vallet et al., 2016) often depending on above-average precipitation over several consecutive years (Bonnard and Noverraz, 2001). Thus, it is usually difficult to establish clear, reliable threshold values of precipitation that cause the activity of deep-seated landslides.

Moreover, although thresholds for Karpenciny are based on a particularly long continuous landslide record, which is significantly longer than the thresholds established till date (Guzzetti et al., 2007, 2008; Segoni et al., 2018), there is still a risk of an unprecedented landslide event caused by precipitation lower than that arising from already existing thresholds. Our analysis conducted at Karpenciny also revealed that the landslide-precipitation relationship can change over time (Figs. 5 and 6), which may affect the performance of all precipitation threshold types, including those based on tree rings. These changes may result from human impact (Garcia-Urquia, 2016; Saito et al., 2017), the transformation of the internal structure of a landslide during its reactivation (Pineda et al., 2016), or changes in climate conditions (Collison et al., 2000; Lopez Saez et al., 2013a). However, the magnitude and direction of changes in slope stability in response to the forecasted climate change and the related change in the activity or frequency of landslides are unclear (Gariano and Guzzetti, 2016). For example, in the temperate climatic zone, where the Karpenciny landslide is located, a shift towards a more uneven annual distribution of precipitation is expected, which would result in alternating periods of extreme rainfall and drought. An increase in evaporation is also forecasted owing to the increase in air temperature. Simultaneously, projected changes in annual precipitation totals are ambiguous (Pińskwar et al., 2019). Moreover, the impact of climate change on landslides depends on the local conditions of slope stability. Although precipitation thresholds of landslide activity will surely vary with climate change, the exact direction of this transformation is difficult to forecast. Thus, the long-term relevance of the presently developed thresholds is uncertain. From this perspective, the dendrochronological long-term records of landslide activity can be considered particularly valuable, as they can reveal how the response of landslides to precipitation has varied in the last few decades within the ongoing climate change.

The analysis conducted in this study has also demonstrated other advantages of precipitation thresholds established from long-term dendrochronological reconstructions of landslides. Based on tree-ring reconstruction, we provided data on precipitation-landslide relationships, including thresholds, for a region where precipitation thresholds of landslide activity are rare (e.g. Gil and Długosz, 2006). According to Guzzetti et al. (2007) and Segoni et al. (2018), data from systematic monitoring and observations of landslide activity are limited or absent in many regions worldwide. Therefore, dendrochronology can help fill this gap and contribute also to threshold calculation.

The analysis of causes for landslide reactivations conducted at Karpenciny consists of an almost 50-year comparison between precipitation records and continuous records of landslide activity, which is significantly longer than landslide datasets commonly available with other methods of monitoring or reconstruction. Moreover, dendrochronology

enabled us to determine precipitation thresholds for a single landslide slope. Such combinations of long datasets with an individual approach to single landslides have been rare in threshold analyses (e.g. Xu et al., 2020). However, such approach is promising as it highlights the local, site-specific causes, which are particularly important in hazard analyses. Moreover, individually determined thresholds reflect the impact of depth, structure, and morphological types of landslides that can differentiate the causes and timing of events even between adjacent slopes (Tong and Schmidt, 2016; Remaître and Malet, 2017; Watakabe and Matsushi, 2019). Likewise, Wistuba et al. (2021) demonstrated that in addition to revealing significant differences in landslide causes, tree-ring analyses also facilitate the determination of similarities in the activity of landslides in one region, that is, shared causes which might be a basis for regional precipitation thresholds.

5. Conclusions

An extended statistical comparison of the 48-year long reconstruction of landslide activity at Karpenciny with numerous precipitation parameters revealed patterns that are significant in establishing precipitation thresholds. The results indicated that landslide activity can depend on long preparatory precipitation from the preceding summer half-years or even before, but primarily of the previous autumn and thaw of present spring. We also demonstrated that the activity of one landslide can be directly caused by more than one factor (in the studied case: spring thaw, precipitation of present summer, and present autumn). Moreover, particular landslide accelerations (events) can correspond to more than one direct cause, all found in the same calendar year. Thus, landslides can begin with one of the revealed causes, continue in the following months, and be enhanced by other factors.

We also determined specific precipitation parameters crucial for the activity of the Karpenciny landslide. The characteristics of these parameters indicate that meteorological conditions favouring landslide acceleration, which are potentially essential for precipitation thresholds, can include the following:

- long-term periods of preparatory precipitation,
- precipitation not occurring below a critical minimum level that sustains slope imbalance,
- generally, wet conditions that are represented by frequent and long-lasting precipitation, regardless of its total.

Consequently, our findings enabled us to develop precipitation thresholds based on both long-term antecedent precipitation and direct triggers. The former can be observed and measured in advance. Thus, it can be used as an early sign of potential landslide reactivation, indicating that further meteorological monitoring should focus on the possible occurrence of a particular direct trigger included in the threshold.

Analysis of precipitation thresholds determined for the Karpenciny landslide revealed the significant potential of the dendrochronological approach in determining:

- landslide-safe conditions, that is, levels of precipitation which have never been related to landslide events,
- levels of precipitation above which landslide reactivation is more probable than maintenance of slope stability.

In particular, thresholds determined from single precipitation parameters encompass the entire relationship between precipitation and diverse levels of landslide activity. However, thresholds determined from pairs of precipitation parameters generally provide a better performance.

The regularity of landslide-precipitation dependence and precipitation thresholds determined in our study would not be revealed with standard methods and standard precipitation parameters applied in threshold analyses. Thus, the dendrochronological approach involving multiple precipitation parameters enabled us to establish precipitation thresholds for the studied unmonitored landslides. Furthermore, it generated extended data on landslide activity and causes that can add to the results of other methods, and aid in understanding landslide responses to meteorological causes of reactivations.

Supplementary data to this article can be found online at https://doi.org/10.1016/j.enggeo.2021.106398.

Declaration of Competing Interest

The authors declare that they have no known competing financial interests or personal relationships that could have appeared to influence the work reported in this paper.

Acknowledgements

This research was supported by the Polish National Science Centre through grant no. 2017/26/D/ST10/00792.

References

Aleotti, P., 2004. A warning system for rainfall-induced shallow failures. Eng. Geol. 73, 247–265. https://doi.org/10.1016/j.enggeo.2004.01.007.

Arghiuş, V.I., Arghiuş, C., Ozunu, A., Nour, E., Roşian, G., Muntean, L.O., 2011. The relation between the landslide activity and irregular rainfall and snowmelt in the Codrului Hills, Romania. Environ. Eng. Manag. J. 10, 3–6. https://doi.org/10.30638/eemj.2011.001.

Behling, R., Roessner, S., Golovko, D., Kleinschmit, B., 2016. Derivation of long-term spatiotemporal landslide activity – a multi-sensor time series approach. Remote Sens. Environ. 186, 88–104. https://doi.org/10.1016/j.rse.2016.07.017.

Bell, F., Maud, R., 2000. Landslides associated with the colluvial soils overlying the Natal Group in the greater Durban region of Natal, South Africa. Environ. Geol. 39, 1029–1038. https://doi.org/10.1007/s002549900077.

Berti, M., Martina, M.L.V., Franceschini, S., Pignone, S., Simoni, A., Pizziolo, M., 2012. Probabilistic rainfall thresholds for landslide occurrence using a Bayesian approach. J. Geophys. Res. 117, F04006 https://doi.org/10.1029/2012JF00236.

Bíl, M., Andrášik, R., Zahradníček, P., Kubeček, J., Sedoník, J., Štěpánek, P., 2016. Total water content thresholds for shallow landslides, Outer Western Carpathians. Landslides 13, 337–347. https://doi.org/10.1007/s10346-015-0570-9.

Błażejczyk, K., 2019. Sezonowa i wieloletnia zmienność niektórych elementów klimatu w Tatrach i Karkonoszach w latach 1951–2015. Przegląd Geograficzny 91 (1), 41–62. https://doi.org/10.7163/PrzG.2019.1.2 (in Polish: Seasonal and multiannual variability of selected elements of climate in the Tatra and Karkonosze Mts over the 1951–2015 period).

Bonnard, C., Noverraz, F., 2001. Influence of climate change on large landslides: assessment of long-term movements and trends. In: International Conference on Landslides – Causes, Impacts and Countermeasures. Davos, Switzerland, pp. 121–138.

Braam, R.R., Weiss, E.E.J., Burrough, P.A., 1987. Spatial and temporal analysis of mass movement using dendrochronology. Catena Suppl. 9, 573–584. https://doi.org/10.1016/0341-8162(87)90007-5.

Brunetti, M.T., Peruccacci, S., Rossi, M., Luciani, S., Valigi, D., Guzzetti, F., 2010. Rainfall thresholds for the possible occurrence of landslides in Italy. Nat. Hazards Earth Syst. Sci. 10, 447–458. https://doi.org/10.5194/nhess-10-447-2010.

Cabon, A., Peters, R.L., Fonti, P., Martínez-Vilalta, J., De Cáceres, M., 2020. Temperature and water potential co-limit stem cambial activity along a steep elevational gradient. New Phytol. 226, 1325–1340. https://doi.org/10.1111/nph.16456.

Caine, N., 1980. The rainfall intensity-duration control of shallow landslides and debris flows. Geografiska Annaler: Series A, Physical Geography 62, 23–27. https://doi.org/10.1080/04353676.1980.11879996.

Campbell, R.H., 1975. Soil slips, debris flows, and rainstorms in the Santa Monica Mountains and vicinity, Southern California. US Geol. Surv. Prof. Pap. 851, 1–51. https://doi.org/10.3133/pp851.

Cardinali, M., Ardizzone, F., Galli, M., Guzzetti, F., Reichenbach, P., 2000. Landslides triggered by rapid snow melting: the December 1996–January 1997 event in Central Italy. In: Proceedings 1st Plinius Conference on Mediterranean Storms. Bios, Cosenza, pp. 439–448.

Carlà, T., Tofani, V., Lombardi, L., Raspini, F., Bianchini, S., Bertolo, D., Thuegaz, P., Casagli, N., 2019. Combination of GNSS, satellite InSAR, and GBInSAR remote sensing monitoring to improve the understanding of a large landslide in high alpine environment. Geomorphology 335, 62–75. https://doi.org/10.1016/j.geomorph.2019.03.014.

Carrara, P.E., O'Neill, J.M., 2003. Tree-ring dated landslide movements and their relationship to seismic events in southwestern Montana, USA. Quat. Res. 59, 25–35. https://doi.org/10.1016/S0033-5894(02)00010-8.

Cebulak, E., 1998. Charakterystyka wysokich opadów wywołujących wezbrania rzek karpackich. Folia Geogr. Ser. Geogr. Phys. 29-30, 43–65 (in Polish: Characteristics of extreme rainfall causing floods of Carpathian rivers).

Chleborad, A.F., 1997. Temperature, Snowmelt, and the Onset of Spring Season Landslides in the Central Rocky Mountains. US Department of the Interior, US Geological Survey, Denver.
Colesanti, C., Wasowski, J., 2006. Investigating landslides with spaceborne synthetic aperture radar (SAR) interferometry. Eng. Geol. 88, 173–199. https://doi.org/10.1016/j.enggeo.2006.09.013.
Collison, A., Wade, S., Griffiths, J., Dehn, M., 2000. Modelling the impact of predicted climate change on landslide frequency and magnitude in SE England. Eng. Geol. 55, 205–218. https://doi.org/10.1016/S0013-7952(99)00121-0.
Corominas, J., Moya, J., 1999. Reconstructing recent landslide activity in relation to rainfall in the Llobregat River basin, Eastern Pyrenees, Spain. Geomorphology 30, 79–93. https://doi.org/10.1016/S0169-555X(99)00046-X.
Cropper, J., 1979. Tree-ring skeleton plotting by computer. Tree-Ring Bull. 39, 47–60.
Crosta, G., Frattini, P., 2001. Rainfall thresholds for triggering soil slips and debris flow. In: Proceedings of EGS 2nd Plinius Conference 2000, Mediterranean Storms. Siena, pp. 463–488.
Crozier, M.J., 1986. Landslides: Causes, Consequences and Environment. Croom Helm, London. https://doi.org/10.7202/032702ar.
Długosz, M., 2011. Podatność stoków na osuwanie w polskich Karpatach fliszowych. IGiPZ PAN, Warszawa (in Polish: Slope susceptibility to landsliding in the Polish Flysch Carpathians).
Eker, R., Aydin, A., 2021. Long-term retrospective investigation of a large, deep-seated, and slow-moving landslide using InSAR time series, historical aerial photographs, and UAV data: the case of Devrek landslide (NW Turkey). Catena 196, 104895. https://doi.org/10.1016/j.catena.2020.104895.
Endo, T., 1969. Probable distribution of the amount of rainfall causing landslides. Annu. Rep. 1968, 122–136.
Fiorucci, F., Cardinali, M., Carlà, R., Rossi, M., Mondini, A.C., Santurri, L., Ardizzone, F., Guzzetti, F., 2011. Seasonal landslide mapping and estimation of landslide mobilization rates using aerial and satellite images. Geomorphology 129, 59–70. https://doi.org/10.1016/j.geomorph.2011.01.013.
Garcia-Urquia, E., 2016. Establishing rainfall frequency contour lines as thresholds for rainfall-induced landslides in Tegucigalpa, Honduras, 1980–2005. Nat. Hazards 82, 2107–2132. https://doi.org/10.1007/s11069-016-2297-x.
Gariano, S.L., Guzzetti, F., 2016. Landslides in a changing climate. Earth Sci. Rev. 162, 227–252. https://doi.org/10.1016/j.earscirev.2016.08.011.
Garland, G.G., Olivier, M.J., 1993. Predicting landslides from rainfall in a humid, sub-tropical region. Geomorphology 8, 165–173. https://doi.org/10.1016/0169-555X(93)90035-Z.
Giannecchini, R., 2005. Rainfall triggering soil slips in the southern Apuan Alps (Tuscany, Italy). Adv. Geosci. 2, 21–24. https://doi.org/10.5194/adgeo-2-21-2005.
Gil, E., Długosz, M., 2006. Threshold values of rainfalls triggering selected deep-seated landslides in the Polish Flysch Carpathians. Studia Geomorphologica Carpatho-Balcanica 40, 21–43.
Glade, T., 2000. Modelling landslide triggering rainfall tresholds at a range of complexities. In: Bromhead, E.N., Dixon, N., Ibsen, M.-L. (Eds.), Landslides in Research, Theory and Practice, Proceedings of the 8th International Symposium on Landslides, Cardiff. Thomas Telford, London, pp. 633–640.
Gorczyca, E., 2010. Slope relaxation following landslides in the Łososina River Basin, Beskid Wyspowy Mts., Poland. Landform Anal. 14, 3–11.
Gorczyca, E., Wrońska-Wałach, D., Długosz, M., 2013. Landslide hazards in the Polish Flysch Carpathians: Example of Łososina Dolna Commune. In: Loczy, D. (Ed.), Geomorphological Impacts of Extreme Weather. Springer Geography. Springer, Dordrecht, pp. 237–250. https://doi.org/10.1007/978-94-007-6301-2_15.
Govi, M., Sorzana, P.F., 1980. Landslide susceptibility as function of critical rainfall amount in Piedmont basin (North-Western Italy). Studia Geomorphologica Carpatho-Balcanica 14, 43–60.
Gullà, G., Calcaterra, S., Gambino, P., Borrelli, L., Muto, F., 2018. Long-term measurements using an integrated monitoring network to identify homogeneous landslide sectors in a complex geo-environmental context (Lago, Calabria, Italy). Landslides 15, 1503–1521. https://doi.org/10.1007/s10346-018-0974-4.
Guzzetti, F., Peruccacci, S., Rossi, M., Stark, C.P., 2007. Rainfall thresholds for the initiation of landslides in central and southern Europe. Meteorog. Atmos. Phys. 98, 239–267. https://doi.org/10.1007/s00703-007-0262-7.
Guzzetti, F., Peruccacci, S., Rossi, M., Stark, C.P., 2008. The rainfall intensity–duration control of shallow landslides and debris flows: an update. Landslides 5, 3–17. https://doi.org/10.1007/s10346-007-0112-1.
He, S., Wang, J., Liu, S., 2020. Rainfall event–duration thresholds for landslide occurrences in China. Water 12, 494. https://doi.org/10.3390/w12020494.
Hong, Y., Hiura, H., Shino, K., Sassa, K., Suemine, A., Fukuoka, H., Wang, G., 2005. The influence of intense rainfall on the activity of large-scale crystalline schist landslides in Shikoku Island, Japan. Landslides 2, 97–105. https://doi.org/10.1007/s10346-004-0043-z.
Jaedicke, C., Kleven, A., 2008. Long-term precipitation and slide activity in South-Eastern Norway, autumn 2000. Hydrol. Processes Int. J. 22, 495–505. https://doi.org/10.1002/hyp.6878.
Kaczka, R.J., Janecka, K., Hulist, A., Spyt, B., 2017. Linking the growth/climate response of daily resolution with annual ring formation of Norway spruce in the Tatra Mountains. TRACE 15, 13–22.
Keck, J., Hsiao, Ch.-Y., Lin, B.-S., Chan, M.-H., Wright, W., 2014. Spatiotemporal landslide activity derived from tree-rings: the Tieliku Mingsui landslide, Northern Taiwan. J. Chin. Soil Water Conserv. 45, 36–48.
Lagomarsino, D., Segoni, S., Fanti, R., Catani, F., 2013. Updating and tuning a regional-scale landslide early warning system. Landslides 10, 91–97. https://doi.org/10.1007/s10346-012-0376-y.
Lopez Saez, J., Corona, C., Stoffel, M., Astrade, L., Berger, F., Malet, J.P., 2012. Dendrogeomorphic reconstruction of past landslide reactivation with seasonal precision: the Bois Noir landslide, southeast French Alps. Landslides 9, 189–203. https://doi.org/10.1007/s10346-011-0284-6.
Lopez Saez, J., Corona, C., Stoffel, M., Berger, F., 2013a. Climate change increases frequency of shallow spring landslides in the French Alps. Geology 41, 619–622. https://doi.org/10.1130/G34098.1.
Lopez Saez, J., Corona, C., Stoffel, M., Berger, F., 2013b. High-resolution fingerprints of past landsliding and spatially explicit, probabilistic assessment of future reactivations: Aiguettes landslide, Southeastern French Alps. Tectonophysics 602, 355–369. https://doi.org/10.1016/j.tecto.2012.04.020.
Łuszczyńska, K., Wistuba, M., Malik, I., Krąpiec, M., Szypuła, B., 2019. Dendrochronological dating as the basis for developing a landslide hazard map – an example from the Western Carpathians, Poland. Geochronometria 45, 173–184. https://doi.org/10.1515/geochr-2015-0093.
Malik, I., Owczarek, P., 2009. Dendrochronological records of debris flow and avalanche activity in a mid-mountain forest zone (Eastern Sudetes – Central Europe). Geochronometria 34, 57–66. https://doi.org/10.2478/v10003-009-0011-7.
Malik, I., Wistuba, M., 2012. Dendrochronological methods for reconstructing mass movements – an example of landslide activity analysis using tree-ring eccentricity. Geochronometria 39, 180–196. https://doi.org/10.2478/s13386-012-0005-5.
Malik, I., Wistuba, M., Migoń, P., Fajer, M., 2016. Activity of slow-moving landslides recorded in eccentric tree rings of Norway spruce trees (Picea abies Karst.) — an example from the Kamienne Mts. (Sudetes Mts., Central Europe). Geochronometria 43, 24–37. https://doi.org/10.1515/geochr-2015-0028.
Malik, I., Poręba, G., Wistuba, M., Woskowicz-Ślęzak, B., 2021. Combining ^{137}Cs, ^{210}Pb and dendrochronology for improved reconstruction of erosion–sedimentation events in a loess gully system (southern Poland). Land Degrad. Dev. 32, 2336–2350. https://doi.org/10.1002/ldr.3903.
Marciniec, P., Zimnal, Z., Wojciechowski, T., Perski, Z., Rączkowski, W., Laskowicz, I., Nieścieruk, P., Grabowski, D., Kułak, M., Wójcik, A., 2019. Osuwiska w Polsce – od rejestracji do prognozy, czyli 13 lat projektu SOPO. Prz. Geol. 67, 291–297 (in Polish: Landslides in Poland: from registration to forecast, 13 years of the LCS project).
Martelloni, G., Segoni, S., Fanti, R., Catani, F., 2012. Rainfall thresholds for the forecasting of landslide occurrence at regional scale. Landslides 9, 485–495. https://doi.org/10.1007/s10346-011-0308-2.
Migoń, P., Kacprzak, A., Malik, I., Kasprzak, M., Owczarek, P., Wistuba, M., Pánek, T., 2014. Geomorphological, pedological and dendrochronological signatures of a relict landslide terrain, Mt Garbatka (Kamienne Mts), SW Poland. Geomorphology 219, 213–231. https://doi.org/10.1016/j.geomorph.2014.05.005.
Owczarek, P., Opała-Owczarek, M., Boudreau, S., Lajeunesse, P., Stachnik, Ł., 2020. Reactivation of landslide in sub-Arctic areas due to extreme rainfall and discharge events (the mouth of the Great Whale River, Nunavik, Canada). Sci. Total Environ. 744, 140991. https://doi.org/10.1016/j.scitotenv.2020.140991.
Palis, E., Lebourg, T., Vidal, M., Levy, C., Tric, E., Hernandez, M., 2017. Multiyear time-lapse ERT to study short- and long-term landslide hydrological dynamics. Landslides 14, 1333–1343. https://doi.org/10.1007/s10346-016-0791-6.
Państwowy Instytut Geologiczny, 2016. Raport z monitoringu wgłębnego. Pomiary inklinometryczne na osuwisku w m. Szaflary. Ministerstwo Środowiska, Kraków (in Polish: Report from underground monitoring. Inclinometer measurements of the landslide in Szaflary).
Papciak, T., Malik, I., Krzemień, K., Wistuba, M., Gorczyca, E., Wrońska-Wałach, D., Sobucki, M., 2015. Precipitation as a factor triggering landslide activity in the Kamień massif (Beskid Niski Mts, Western Carpathians). Bulletin of Geography. Phys. Geogr. Ser. 8, 5–17. https://doi.org/10.1515/bgeo-2015-0001.
Pelfini, M., Santilli, M., 2008. Frequency of debris flows and their relation with precipitation: a case study in the Central Alps, Italy. Geomorphology 101, 721–730. https://doi.org/10.1016/j.geomorph.2008.04.002.
Peruccacci, S., Brunetti, M.T., Luciani, S., Vennari, C., Guzzetti, F., 2012. Lithological and seasonal control of rainfall thresholds for the possible initiation of landslides in central Italy. Geomorphology 139-140, 79–90. https://doi.org/10.1016/j.geomorph.2011.10.005.
Peruccacci, S., Brunetti, M.T., Gariano, S.L., Melillo, M., Rossi, M., Guzzetti, F., 2017. Rainfall thresholds for possible landslide occurrence in Italy. Geomorphology 290, 39–57. https://doi.org/10.1016/j.geomorph.2017.03.031.
Pennington, C., Dijkstra, T., Lark, M., Dashwood, C., Harrison, A., Freeborough, K., 2014. Antecedent precipitation as a potential proxy for landslide incidence in south west United Kingdom, in: Sassa, K., Canuti, P., Yin, Y. (Eds.), Landslide Science for a Safer Geoenvironment 1. Springer, Cham, pp. 253-259. https://doi.org/10.1007/978-3-319-04999-1_34.
Pineda, M.C., Viloria, J., Martínez-Casasnovas, J.A., 2016. Landslides susceptibility change over time according to terrain conditions in a mountain area of the tropic region. Environ. Monit. Assess. 188, 255. https://doi.org/10.1007/s10661-016-5240-4.
Pińskwar, I., Choryński, A., Graczyk, D., Kundzewicz, Z.W., 2019. Observed changes in extreme precipitation in Poland: 1991–2015 versus 1961–1990. Theor. Appl. Climatol. 135, 773–787. https://doi.org/10.1007/s00704-018-2372-1.
Piotrowska, K., Rączkowski, W., Iwanow, A., Zabielski, R., Derkacz, M., Wójcik, A., Michalik, M., Wasiluk, R., 2017. Szczegółowa mapa geologiczna 1:50 000. 1061 – Tatry Wysokie (M-34-101-A). Państwowy Instytut Geologiczny, Ministerstwo Środowiska, Warszawa (in Polish: Detailed geological map 1:50 000. 1060 – The High Tatra Mts (M-34-101-A)).
Poprawa, D., Rączkowski, W., 2003. Osuwiska Karpat. Prz. Geol. 51, 685–692 (in Polish: Landslides of the Carpathian Mts).

Prokešová, R., Medveďová, A., Tábořík, P., Snopková, Z., 2012. Towards hydrological triggering mechanisms of large deep-seated landslides. Landslides 10, 239–254. https://doi.org/10.1007/s10346-012-0330-z.
Rączkowski, W., 2007. Landslide hazard in the Polish Flysch Carpathians. Studia Geomorphologica Carpatho-Balcanica 41, 61–75.
Rączkowski, W., 2014. Objaśnienia do mapy osuwisk i terenów zagrożonych ruchami masowymi. Skala 1:10000, Gmina Zakopane, Powiat tatrzański, Województwo małopolskie. Państwowy Instytut Geologiczny – Państwowy Instytut Badawczy. Warszawa (in Polish: Explanations for the map of landslides and areas endangered by mass movements. Scale 1:10000, Zakopane Commune, tatrzański district, Małopolskie Province).
Remaître, A., Malet, J.-P., 2017. Regional rainfall thresholds for shallow and deep-seated mass movements triggering in the south eastern French Alps. In: Mikoš, M., Casagli, N., Yin, Y., Sassa, K. (Eds.), Advancing Culture of Living with Landslides. WLF 2017. Springer, Cham, pp. 183–192. https://doi.org/10.1007/978-3-319-53485-5_20.
Rosi, A., Lagomarsino, D., Rossi, G., Segoni, S., Battistini, A., Casagli, N., 2015. Updating EWS rainfall thresholds for the triggering of landslides. Nat. Hazards 78, 297–308. https://doi.org/10.1007/s11069-015-1717-7.
Ruelle, J., 2014. Morphology, Anatomy and Ultrastructure of Reaction Wood. In: Gardiner, B., Barnett, J., Saranpää, P., Gril, J. (Eds.), The Biology of Reaction Wood. Springer, Berlin, Heidelberg, pp. 13–35. https://doi.org/10.1007/978-3-642-10814-3.
Saito, H., Murakami, W., Daimaru, H., Oguchi, T., 2017. Effect of forest clear-cutting on landslide occurrences: Analysis of rainfall thresholds at Mt. Ichifusa, Japan. Geomorphology 276, 1–7. https://doi.org/10.1016/j.geomorph.2016.09.024.
Segoni, S., Rosi, A., Rossi, G., Catani, F., Casagni, N., 2014a. Analysing the relationship between rainfalls and landslides to define a mosaic of triggering thresholds for regional scale warning systems. Nat. Hazards Earth Syst. Sci. 14, 2637–2648. https://doi.org/10.5194/nhess-14-2637-2014.
Segoni, S., Rossi, G., Rosi, A., Catani, F., 2014b. Landslides triggered by rainfall: a semiautomated procedure to define consistent intensity-duration thresholds. Comput. Geosci. 63, 123–131. https://doi.org/10.1016/j.cageo.2013.10.009.
Segoni, S., Piciullo, L., Gariano, S.L., 2018. A review of the recent literature on rainfall thresholds for landslide occurrence. Landslides 15, 1483–1501. https://doi.org/10.1007/s10346-018-0966-4.
Shroder Jr., J.F., 1978. Dendrogeomorphological analysis of mass movement on Table Cliffs Plateau, Utah. Quat. Res. 9, 168–185. https://doi.org/10.1016/0033-5894(78)90065-0.
Šilhán, K., Pánek, T., Hradecký, J., 2012. Tree-ring analysis in the reconstruction of slope instabilities associated with earthquakes and precipitation (the Crimean Mountains, Ukraine). Geomorphology 173-174, 174–184. https://doi.org/10.1016/j.geomorph.2012.06.010.
Szabó, J., 2003. The relationship between landslide activity and weather: examples from Hungary. Nat. Hazards Earth Syst. Sci. 3, 43–52. https://doi.org/10.5194/nhess-3-43-2003.
Szczygieł, J., Mendecki, M., Hercman, H., Wróblewski, W., Glazer, M., 2019. Relict landslide development as inferred from speleothem deformation, tectonic data, and geoelectrics. Geomorphology 330, 116–128. https://doi.org/10.1016/j.geomorph.2019.01.017.
Timell, T.E., 1986. Compression Wood in Gymnosperms. Springer−Verlag, New York.
Tong, X., Schmidt, D., 2016. Active movement of the Cascade landslide complex in Washington from a coherence-based InSAR time series method. Remote Sens. Environ. 186, 405–415. https://doi.org/10.1016/j.rse.2016.09.008.
Vallet, A., Varron, D., Bertrand, C., Fabbri, O., Mudry, J., 2016. A multi-dimensional statistical rainfall threshold for deep landslides based on groundwater recharge and support vector machines. Nat. Hazards 84, 821–849. https://doi.org/10.1007/s11069-016-2453-3.
Wasowski, J., Pisano, L., 2020. Long-term InSAR, borehole inclinometer, and rainfall records provide insight into the mechanism and activity patterns of an extremely slow urbanized landslide. Landslides 17, 445–457. https://doi.org/10.1007/s10346-019-01276-7.
Watakabe, T., Matsushi, Y., 2019. Lithological controls on hydrological processes that trigger shallow landslides: Observations from granite and hornfels hillslopes in Hiroshima, Japan. Catena 180, 55–68. https://doi.org/10.1016/j.catena.2019.04.010.
Weidner, L., DePrekel, K., Oommen, T., Vitton, S., 2019. Investigating large landslides along a river valley using combined physical, statistical, and hydrologic modeling. Eng. Geol. 259, 105169. https://doi.org/10.1016/j.enggeo.2019.105169.
Wiedenhoeft, A.C., 2013. Structure and function of wood. In: Rowell, R.M. (Ed.), Handbook of Wood Chemistry and Wood Composites. CRC Press Taylor and Francis Group, Boca Raton, pp. 9–32.
Wistuba, M., 2014. Slope-Channel Coupling as a Factor in the Evolution of Mountains. The Western Carpathians and Sudetes. Springer International Publishing, Cham, Heidelberg, New York, Dordrecht, London. https://doi.org/10.1007/978-3-319-05819-1.
Wistuba, M., Malik, I., Gärtner, H., Kojs, P., Owczarek, P., 2013. Application of eccentric growth of trees as a tool for landslide analyses: the example of *Picea abies* Karst. in the Carpathian and Sudeten Mountains (Central Europe). Catena 111, 41–55. https://doi.org/10.1016/j.catena.2013.06.027.
Wistuba, M., Malik, I., Wójcicki, K., Michałowicz, P., 2015. Coupling between landslides and eroding stream channels reconstructed from spruce tree rings (examples from the Carpathians and Sudetes – Central Europe). Earth Surf. Process. Landf. 40, 293–312. https://doi.org/10.1002/esp.3632.
Wistuba, M., Malik, I., Krzemień, K., Gorczyca, E., Sobucki, M., Wrońska-Wałach, D., Gawior, D., 2018. Can low-magnitude earthquakes act as a triggering factor for landslide activity? Examples from the Western Carpathian Mts, Poland. Catena 171, 359–375. https://doi.org/10.1016/j.catena.2018.07.028.
Wistuba, M., Malik, I., Badura, J., 2019. Tree rings as an early warning against catastrophic landslides: Assessing the potential of dendrochronology for determining slope stability. Dendrochronologia 53, 82–94. https://doi.org/10.1016/j.dendro.2018.12.002.
Wistuba, M., Malik, I., Gorczyca, E., Ślęzak, A., 2021. Establishing regimes of landslide activity – Analysis of landslide triggers over the previous seven decades (Western Carpathians, Poland). Catena 196, 104888. https://doi.org/10.1016/j.catena.2020.104888.
Xu, Y., Lu, Z., Schulz, W.H., Kim, J., 2020. Twelve-year dynamics and rainfall thresholds for alternating creep and rapid movement of the Hooskanaden landslide from integrating InSAR, pixel offset tracking, and borehole and hydrological measurements. J. Geophys. Res. Earth Surf. 125 https://doi.org/10.1029/2020JF005640 e2020JF005640.
Yang, H., Wei, F., Ma, Z., Guo, H., Su, P., Zhang, S., 2020. Rainfall threshold for landslide activity in Dazhou, southwest China. Landslides 17, 61–77. https://doi.org/10.1007/s10346-019-01270-z.
Yumoto, M., Ishida, S., Fukazawa, K., 1983. Studies on the formation and structure of the compression wood cells induced by artificial inclination in young trees of Picea glauca. IV. Gradation of the severity of compression wood tracheids. Res. Bull. College Exp. Forests 40, 409–454.
Zêzere, J.L., 2000. Rainfall triggering of landslides in the area north of Lisbon. In: Bromhead, E.N., Dixon, N., Ibsen, M.-L. (Eds.), Landslides in Research, Theory and Practice, Proceedings of the 8th International Symposium on Landslides, Cardiff. Thomas Telford, London, pp. 1629–1634.
Zhang, W.J., Chen, Y.M., Zhan, L.T., 2006. Loading/unloading response ratio theory applied in predicting deep-seated landslides triggering. Eng. Geol. 82, 234–240. https://doi.org/10.1016/j.enggeo.2005.11.005.
Zhao, B., Dai, Q., Han, D., Dai, H., Mao, J., Zhuo, L., 2019. Probabilistic thresholds for landslides warning by integrating soil moisture conditions with rainfall thresholds. J. Hydrol. 574, 276–287. https://doi.org/10.1016/j.jhydrol.2019.04.062.